Available online at www.sciencedirect.com
SCIENCE DIRECT
Precambrian Research 145 (2006) 111–130
Precambrian Research
www.elsevier.com/locate/precamres

LA-ICP-MS U-Pb zircon geochronology of the Neoproterozoic igneous rocks from Northern Guangxi, South China: Implications for tectonic evolution

Xiao-Lei Wang [a], Jin-Cheng Zhou [a,*], Jian-Sheng Qiu [a], Wen-Lan Zhang [a], Xiao-Ming Liu [b], Gui-Lin Zhang [c]

[a] *State Key Laboratory for Mineral Deposits Research, Department of Earth Sciences, Nanjing University, Nanjing 210093, PR China*
[b] *Department of Geology, Northwest University, Xi'an 710069, PR China*
[c] *Department of Resource and Environmental Engineering, Guilin Institute of Technology, Guilin 541004, PR China*

Received 22 March 2005; received in revised form 19 October 2005; accepted 16 November 2005

Abstract

The western end of the Proterozoic Jiangnan orogen is located at the Northern Guangxi, South China. Neoproterozoic granitoids are dominant (>90%) in the area, with ca. 8% being the mafic-ultramafic rocks. The generation of these igneous rocks was previously considered to be related to a mantle plume (or superplume) event that led to the breakup of the Rodinia supercontinent. In this work, we present new laser ablation-ICP-MS U-Pb zircon data for the igneous rocks from Northern Guangxi. The ages for the Zhaigun, Bendong, Dongma, Sanfang and Tianpeng granitic plutons are 835.8 ± 2.5, 822.7 ± 3.8, 824 ± 13, 804.3 ± 5.2 and 794.2 ± 8.1 Ma, respectively, and the Hejiawan layered diabases are 811.5 ± 4.8 Ma. These ages indicate a broad duration of magmatic activities (ca. 35 million years), inconsistent with plume models that predict widespread magmatic eruption and emplacement within period of 1–5 million years. The granitoids in Northern Guangxi are typical S-type granites with high ACNK values (1.10–1.87), and are generally plotted in the collision-related areas in the tectonic discrimination diagrams. They should not be the products of the mantle plume activity. On the contrary, they might be related with the continent–continent collisional orogeny between the Yangtze and Cathysia blocks. A total of eight spot analyses of zircon cores and two from single zircon xenoliths gave early Neoproterozoic ages ranging from ca. 870–950 Ma. These ages might record subduction or collision-related magmatic events during 950–870 Ma in Northern Guangxi. Combined with previous geochronological and geochemical data, our new dating results support post-collisional extension, instead of mantle plume or superplume model, for the genesis of 835–800 Ma granites and mafic rocks in Northern Guangxi. The upwelling of deep mantle due to the detachment of subducted slab and the delamination of the lithosphere might cause partial melting of the continental crust to generate S-type granites. The continent–continent collisional orogenic event along the Jiangnan orogen may have spanned ca. 70 million years from 870 to 800 Ma, and the early Neoproterozoic subduction might last for ca. 130 million years. It is proposed that South China might have been located at the western margin in the Rodinia supercontinent during the period of ca. 870–800 Ma.

Keywords: LA-ICP-MS U-Pb zircon dating; Igneous rocks; Post-collisional; Neoproterozoic; Northern Guangxi of South China

1. Introduction

In the last decade, the Precambrian evolution of South China during the formation and breakup of the Rodinia supercontinent has been a focus of much debate and

* Corresponding author. Tel.: +86 25 83686336; fax: +86 25 83686016.
E-mail address: j.c.zhou@public1.ptt.js.cn (J.-C. Zhou).

0301-9268/$ – see front matter © 2005 Elsevier B.V. All rights reserved.
doi:10.1016/j.precamres.2005.11.014

controversy (Evans et al., 2000; Li XH et al., 2003; Li ZX et al., 1995, 1999, 2003, 2004; Zhao and Cawood, 1999; Zheng, 2004; Zhou et al., 2002, 2004; Wang et al., 2004a,b). It was suggested that South China lay between the eastern side of the Australian craton and the western side of Laurentia and might be an important element in the reconstruction of the Rodinia supercontinent (Li et al., 1995). Based on geochronology for the mafic to ultramafic dykes from Northern Guangxi Province of South China and correlations with the Gairdner Dyke Swarm (GDS) in central-southern Australia, Li et al. (1999) proposed that a mantle plume centered beneath South China initiated the rifting of Rodinia at about 820 million years ago. A more comprehensive superplume model was recently proposed by Li ZX et al. (2003, 2004) to explain the breakup of Rodinia. However, the mantle plume hypothesis has been questioned by several authors (Yan et al., 2002; Jiang et al., 2003; Wang et al., 2004a,b; Zhou et al., 2002, 2004).

The Neoproterozoic igneous rocks of South China, especially those distributed along the southeastern margin of the Yangtze Block (or the 'Jiangnan orogen'; Fig. 1a), became the key to understanding the evolution of South China at this time. Two possible explanations for their genesis and tectonic settings are: (1) the coeval and bimodal magmatism was initiated by a mantle plume

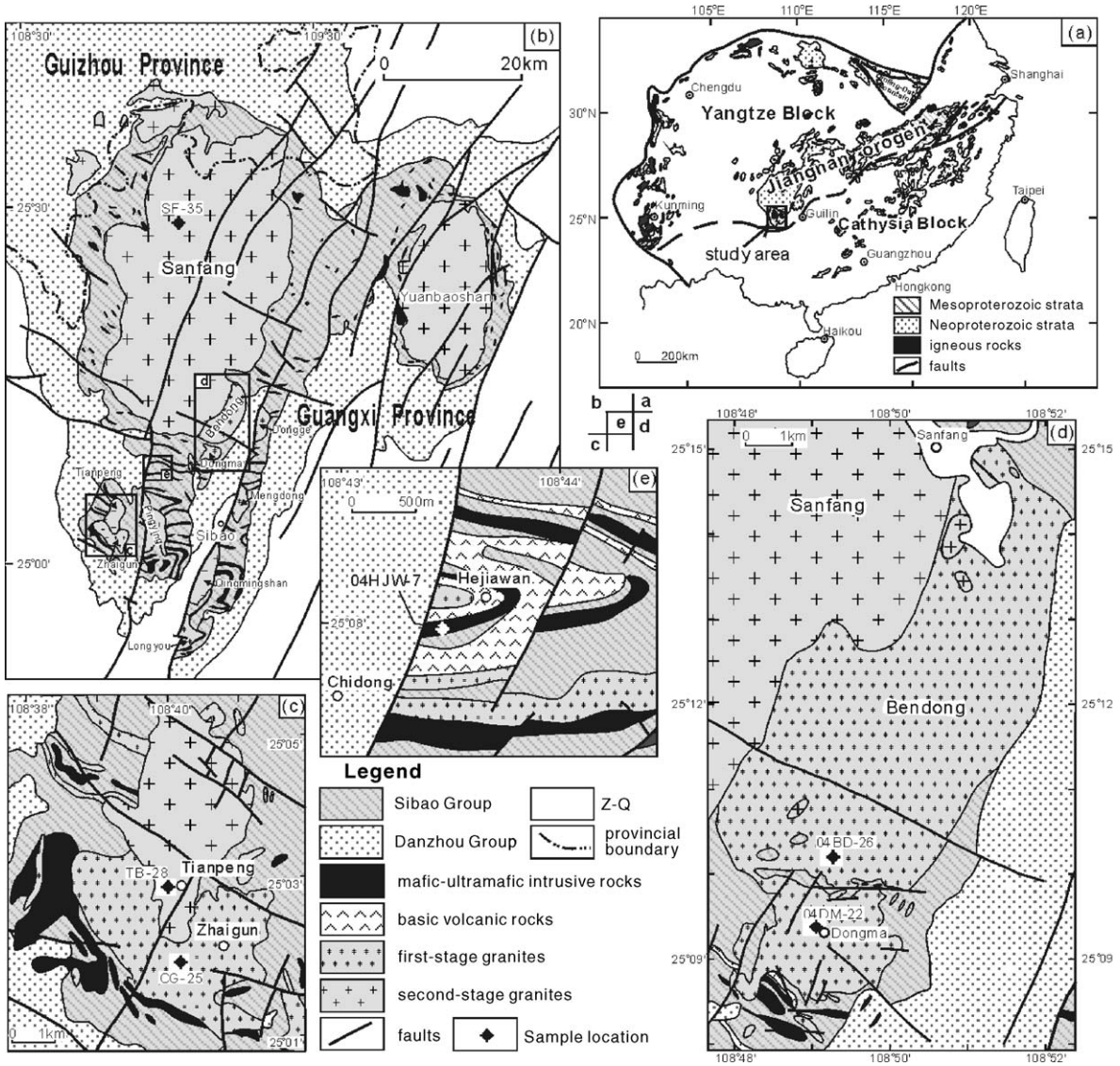

Fig. 1. Geological map of the igneous rocks from Northern Guangxi, South China (modified after GXRGST, 1987, 1995; Chen et al., 1995; Wang, 2000). (a) South China; (b) Northern Guangxi; (c) Tianpeng and Zhaigun plutons; (d) Bendong and Dongma plutons; (e) Hejiawan bedding diabase.

or superplume (Li XH et al., 2003; Li ZX et al., 1999, 2003, 2004); and (2) the Neoproterozoic igneous rocks were generated from the subduction of oceanic crust and the collision between the Cathysia and Yangtze blocks (Guo et al., 1980; Chen et al., 1991; Xu et al., 1992; Xu and Zhou, 1992; Zhou and Zhu, 1993; Li, 1999; Wang et al., 2004b; Zhou et al., 2004). In this work, we have determined the ages for a suit of Neoproterozoic granitoids and a mafic rock from Northern Guangxi of South China. Major, trace element and Sr-Nd isotopic data of the granitoids are also presented. Based on our new laser ablation (LA)–ICP-MS U-Pb zircon geochronological results and the available geochemical data, an alternative model accounting for the Neoproterozoic magmatism and tectonic evolution of South China is presented.

2. Geological setting

South China, separated from the North China Craton by the Qinling-Dabie Mountains, comprises the Yangtze Block in the northwest and the Cathaysia Block in the southeast (Fig. 1a). The Jiangnan orogen, in which the Proterozoic strata and voluminous igneous rocks are dominant, is located along the southeastern margin of the Yangtze Block (Fig. 1a). The western end of the Proterozoic Jiangnan orogen is located at the northern Guangxi, South China. The Proterozoic strata in Northern Guangxi comprise two low-grade greenschist-facies metamorphosed sequences separated by an unconformity, marking the boundary between the Meso- and Neoproterozoic. The Mesoproterozoic Sibao Group, equivalent to the Lengjiaxi Group in Hunan Province and the Shuangqiaoshan Group in Jiangxi Province, constitutes the basement of the Jiangnan orogen. It consists of bathy-abyssal sandy-argillaceous terrigenous sedimentary with flysch bedding and metamorphosed mafic-ultramafic volcanic intercalations, such as tholeiite, spilite with pillow structure, and volcaniclastic rocks (BGMRGX, 1985; GXRGST, 1987, 1995). The Neoproterozoic Danzhou Group, equivalent to the Banxi Group in Hunan Province and the Dengshan Group in Jiangxi Province, includes pelitic-silty rocks with flysch rhythm and Bouma sequence, lesser carbonate rocks, spilite and volcaniclastic rocks (BGMRGX, 1985). The Sibao Group shows tight linear folds trending NE to nearly EW, in response to the northward subduction of oceanic crust, whereas the overlying Danzhou Group shows broad folds (BGMRGX, 1985). This study focuses on the igneous rocks from the Baotan, Sanfang and Yuanbaoshan areas of Northern Guangxi (Fig. 1a and b).

2.1. Granitoids

The granitoids, with more than 13 plutons, are about 92% of the Precambrian igneous rocks (total area of ca. 1685 km^2) exposed in Northern Guangxi (Zhao et al., 1987). The distributions of the granitic plutons are basically controlled by the NNE faults and the E-W trending Sibao Group (Fig. 1b). They intruded the Mesoproterozoic Sibao Group, and have been previously considered to be the products of two different magmatic events (Fig. 1b; GXRGST, 1987). The first-stage granitoids are mostly granodiorites, including the Bendong (~40 km^2), Dongma (~4 km^2), Zhaigun (~11 km^2), Dazhai (~2.5 km^2) and Longyou (~8 km^2) plutons (GXRGST, 1987). The second-stage ones, dominated by biotite granites, mainly consist of the Sanfang (~1000 km^2), Pingying (~18 km), Tianpeng (~10 km^2), and Yuanbaoshan (~300 km^2) plutons (GXRGST, 1987, 1995). Compared with the first-stage plutons, the second-stage granites are relatively coarse-grained, light in color, and tourmalinization is generally encountered in them.

The Tianpeng pluton, which has been considered to be closely related with the tin-polymetal mineralization (Chen et al., 1995), intruded the Zhaigun pluton (Fig. 1c). A five-point Rb-Sr whole rock isochron age of 952 ± 86 Ma for the Tianpeng pluton has been obtained (GXRGST, 1987), but with an especially low initial $^{87}Sr/^{86}Sr$ ratio of 0.614. The Zhaigun pluton intruded in the mafic-ultramafic rocks of the Sibao Group in its southern and western flanks (Fig. 1c; GXRGST, 1987). The Sanfang pluton, dominantly composed of coarse-grained biotite granite, intruded the Bendong pluton (Fig. 1d and Fig. 2a and b). The Bendong pluton, with a kidney shape, is mainly composed of medium to fine-granular granodiorites, and is overlain by the pebble-bearing argillaceous sandstones of the Neoproterozoic Danzhou Group (Fig. 2c). Li (1999) reported two indistinguishable SHRIMP U-Pb zircon ages, 826 ± 10 Ma for the Sanfang and 819 ± 9 Ma for the Bendong plutons. Some of the pebbles in the sandstones have similar composition with the Bendong granites (GXRGST, 1995), suggesting that the lower boundary age of the Danzhou Group is younger than that of the Bendong pluton. The Dongma pluton is located to the south of the Bendong pluton and intruded the mafic-ultramafic rocks in the Sibao Group (Fig. 1d).

2.2. Mafic-ultramafic rocks

The mafic-ultramafic rocks in the Baotan, Sanfang and Yuanbaoshan areas of Northern Guangxi, with a

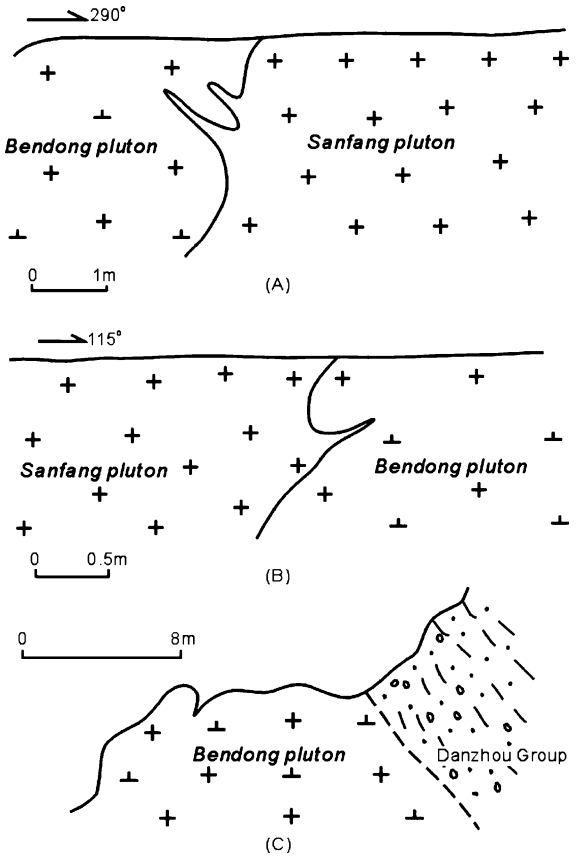

Fig. 2. Field sketch figures showing the intrusion and overlying relationship between Sanfang, Bendong plutons and the Danzhou Group (modified after GXRGST, 1995). (a) The Sanfang pluton intruded the Bendong pluton at the west Sanfang town; (b) The Sanfang pluton intruded the Bendong pluton at the southwest Sanfang town; (c) The Bendong pluton are overlain by the pebble-bearing sandstone of the lower part of the Danzhou Group near the Sanfang town.

total crop area of less than 140 km^2 (BGMRGX, 1985; GXRGST, 1987, 1995; Chen et al., 1995), occur generally as lenses and sills sub-parallel to the structural trend of the Sibao Group, with a few being irregular intrusions (Fig. 1b). There are over 300 exposures of the mafic-ultramafic rocks, some of which are in turn truncated by the granite intrusions (Fig. 1b; BGMRGX, 1985; GXRGST, 1987, 1995). Tremolitization is common in these mafic-ultramafic rocks. Komatiitic basalts interbedded with sedimentary rocks of the Sibao Group have been reported in the Baotan area (GXRGST, 1987; Yang, 1990; Zhou et al., 2000), but their komatiitic features have been questioned (Ge et al., 2001b). Diabases are common in the Baotan area. One layered diabase, located at ca. 350 m southwest of the Hejiawan village, was selected to study in this work (Fig. 1e). It intruded the Mesoproterozoic Sibao Group with the layering parallel to the country rocks (Fig. 1e). The layered diabase has been previously regarded as a part of the Sibao Group (GXRGST, 1987). A layered mafic volcanic rock body, which has been regarded as komatiitic basalts (Zhou et al., 2000), is spatially associated with this layered diabase (Fig. 1e).

Ages of the mafic-ultramafic rocks in the area are still of great debate. Han et al. (1994) obtained an Sm-Nd whole rock isochron age of 1782 ± 82 Ma for the mafic-ultramafic rocks and zircon $^{207}Pb/^{206}Pb$ evaporation ages ranging from 1734 ± 20 to 1863 ± 7 Ma for the pillow basalts from the Sibao Group in the Baotan area. Re-Os isotope age of Cu-Ni sulphide ore hosted in the Sibao Group is 982 ± 21 Ma (Mao and Du, 2001). The mafic-ultramafic dykes from the Yangmeiao county (near northern margin of the Baotan area), that intruded the Sibao Group and are truncated by the Sanfang pluton (U-Pb zircon age of 826 ± 10 Ma; Li, 1999) and overlain by the Baizhu Formation of the Danzhou Group, have a mean SHRIMP U-Pb zircon age of 828 ± 7 Ma (Li et al., 1999). All data of the scattered ages (ranging from 828 to 1863 Ma) for the mafic-ultramafic rocks in Northern Guangxi imply numerous magmatic events, and more precise geochronological data are necessary.

3. Sampling and analytical methods

We selected five representative granitic plutons (i.e. Zhaigun, Bendong, Dongma, Sanfang and Tianpeng plutons) that intruded the Sibao Group and a layered diabase near Hejiawan village for LA-ICP-MS U-Pb zircon dating. Sampling locations are shown in Fig. 1.

All of the samples from the five granitic plutons/one diabase intrusion for dating are fresh without deformation. Zircons were separated using conventional heavy liquid and magnetic techniques, mounted in epoxy resin and polished down to expose the grain centers. The selection of zircons for isotopic analyses was done on the basis of the backscatter electron (BSE) and Cathodoluminescence (CL) images (Fig. 3). BSE investigation was performed on an electron microprobe (JEOL JXA-8800M) hosted at the Electron Microprobe Center, Department of Earth Sciences, Nanjing University (NJU). CL photos were acquired with a scanning electron microscope (XL30 SFEG SEM) at the Department of Electronics, Peking University. Most of the selected zircons are euhedral and colorless.

U-Pb zircon dating was carried out at the State Key Laboratory of Continental Dynamics, Northwest University, Chinese Ministry of Education. The ICP-MS used in this study is ELAN6100DRC from Perkin-Elmer/SCIEX

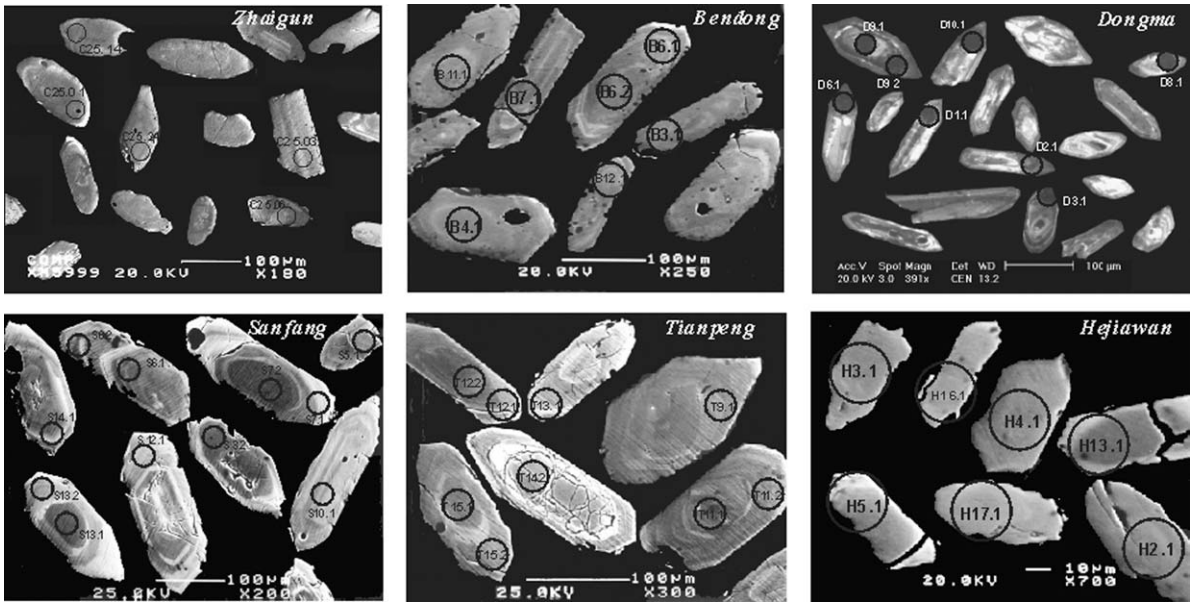

Fig. 3. Representative BSE and CL images of zircon grains. BSE for the Zhaigun, Bendong, Sanfang and Tianpeng granitic plutons and the Hejiawan bedding diabase; CL for the Dongma plutons. Circles indicate analyzed spots.

(Ont., Canada) with a dynamic reaction cell (DRC) and Agillent 7500a. The GeoLas 200M laser-ablation system (MicroLas, Göttingen, Germany) was used for laser-ablation experiments. The system is equipped with a 193 nm ArF-excimer laser from Lambda Physik with a homogenizing, imaging optical system designed by Prof. Detlef Günther. Analytical processes are similar to those of Yuan et al. (2003).

All U-Th-Pb isotope measurements were performed using zircon 91500 as an external standard for age calculation (Wiedenbeck et al., 1995) and NIST SRM 610 as the external standard for the concentration calculation in conjunction with the internal standardization ^{29}Si (32.8% Si in zircon). To test the validity of the results, one spot analysis for the international standard TEM was done at the beginning and the end of analyzing process of every sample. Results of this work suggest that the TEM spot analyses are coincided with each other, and they yielded a weighted average ^{206}Pb/^{238}U age of 417 + 1/−1 Ma, corresponding to its ^{206}Pb/^{238}U age of 417 Ma very well.

Two spot sizes were applied according to the sizes of the zircon grains: 40 μm for the Bendong granite and 30 μm for the other samples. Isotopic ratios and U, Th, and Pb concentrations were calculated using GLITER 4.0 (Macquarie University) while the age calculation and plotting of concordia diagrams were made using Isoplot program (ver 2.49) (Ludwig, 1991). Concentration values of NIST SRM 610 used for the external calibration are taken from Pearce et al. (1997). Because the ^{207}Pb/^{206}Pb are sensative to the common Pb corrections, the ^{206}Pb/^{238}U age is normally adopted for the comparatively young rocks (younger than about 1000 Ma) (Black et al., 2003). In this work, two samples show a horizontal arrangement in ^{206}Pb/^{238}U versus ^{207}Pb/^{235}U plots (Fig. 4). This might be resulted from the analytical uncertainty in ^{207}Pb (Yuan et al., 2003) and trace common lead contamination, possibly due to ablation of epoxy mounting the zircon grains (Jackson et al., 2004). However, no common lead correction was applied for most samples due to the very low ^{204}Pb counts and its poor analytical precision. As revealed by the analytical results of the standard TEM, the trace common lead could not affect the ^{206}Pb/^{238}U ages evidently. The ^{206}Pb/^{238}U ages, with a relatively high precise and stability, also did not be affected by the ^{207}Pb, and could be used to calculate the crystallization ages for the samples.

Major elements were analyzed using a VF-320 X-ray fluorescence spectrometer (XRF) at the Center of Modern Analysis, NJU, following the procedures described by Franzini et al. (1972). The analytical precision is generally less than 2%. Rare earth and other trace elements were analyzed using ICP-AES (JY38S) and ICP-MS (Finnigan MAT-Element 2) techniques at the State Key Laboratory for Mineral Deposits Research, NJU. Procedures for ICP-AES are similar to those of Liu et al. (1999) and Zhu et al. (2001), with a relative accuracy of 5–10%. Analytical precision for most elements by ICP-

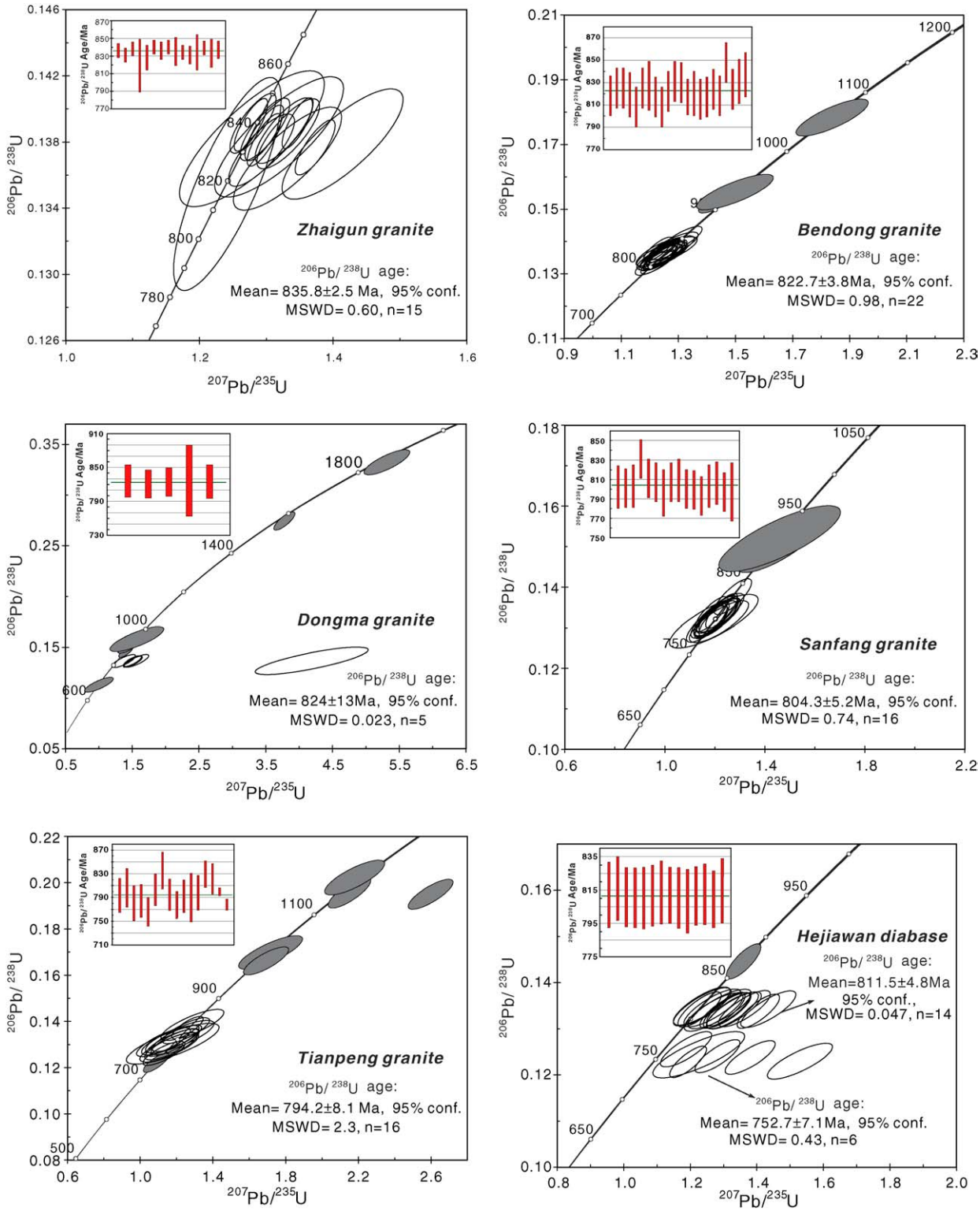

Fig. 4. Zircon U-Pb concordia plots and recalculated weighted mean $^{206}Pb/^{238}U$ ages for the different samples from the Zhaigun, Bendong, Dongma, Sanfang and Tianpeng plutons and the Hejiawan diabase.

MS is better than 5% with analytical procedures similar to Wang et al. (2004b).

Sr-Nd isotopes were analyzed using the ID-TIMS method by a multi-collector Finnigan MAT-261 mass spectrometer operated in static multi-collector mode at the Isotope Laboratory of the China University of Geosciences. Analytical procedures are similar to Ling et al. (2003) and Ye et al. (2001). Analytical precisions for $^{87}Rb/^{86}Sr$ and $^{87}Sr/^{86}Sr$ are better than 0.5 and 0.004%, respectively. The $^{87}Sr/^{86}Sr$ ratio of standard NBS987 is 0.710319 ± 19. Analytical precisions for $^{147}Sm/^{144}Nd$ and $^{143}Nd/^{144}Nd$ are better than 0.1 and 0.002%, respectively. The determined $^{143}Nd/^{144}Nd$ ratios of standard La Jolla and standard basalt GBW04419-02 are 0.511862 ± 4 and 0.512744 ± 14, respectively. The Nd model ages are calculated following the formulation of two-stage Nd model age of Li XH et al. (2003).

4. U-Pb dating

4.1. Sample CG-25, Zhaigun granite

Sample CG-25, a fine-grained granodiorite, is composed of andesine, K-feldspar, quartz and biotite, and has undergone slight sericitization and zoisitization. Zircons are light red to transparent, euhedral, stubby prismatic grains and have magmatogenic oscillatory zoning (Fig. 3). They generally range up to 80–180 μm in length and 40–60 μm in width. Fifteen analyses were obtained, and were corrected according to the program of Andersen (2002). The corrected analytical results are listed in Table 1. The Th/U ratios of the zircons from the sample range from 0.39 to 1.08 (Table 1). All of the analyses are concordant and yield a weighted average $^{206}Pb/^{238}U$ age of 835.8 ± 2.8 Ma (95% confidence, MSWD = 0.6; Fig. 4), which is interpreted as the crystallization age of the Zhaigun pluton.

4.2. Sample 04BD-26, Bendong granite

Sample 04BD-26, a medium to fine-grained granodiorite, is composed of andesine, quartz, K-feldspar and biotite, and has similarly undergone sericitization and zoisitization like sample CG-25. Zircons in this sample are light yellow to transparent, euhedral, stubby prismatic grains (Fig. 3) and have magmatogenic oscillatory zoning with Th/U ratios in the range of 0.11–0.70 (Table 1). In Fig. 4, all of the spot analyses spread along the concordia. In three spots from zircon cores, one gives a late Mesoproterozoic age (B1.1, $^{207}Pb/^{206}Pb$ age of 1057 ± 13 Ma), and the other two yield early Neoproterozoic ages (i.e. the $^{206}Pb/^{238}U$ ages of B18.1 is 918 ± 10 Ma and the B23.1 is 930 ± 12 Ma). The remaining 22 analyses fall within a group, and yield a weighted mean $^{206}Pb/^{238}U$ age of 822.7 ± 3.8 Ma (95% confidence, MSWD = 0.98), in agreement with the SHRIMP U-Pb zircon age of 819 ± 9 Ma ($n = 13$) reported by Li (1999). The age of 822.7 ± 3.8 Ma is considered to represent the crystallization age of the Bendong pluton.

4.3. Sample 04DM-22, Dongma granite

Sample 04DM-22, a fine-grained granodiorite, is composed of plagioclase ($An_{23–25}$), quartz, K-feldspar and biotite with slight sericite and zoisite alteration. This sample was selected to examine whether Mesoproterozoic granites exist in Northern Guangxi. Sizes of the zircon grains in this granite are smaller than those of the sample 04BD-26 of the Bendong pluton. Euhedral, short prismatic zircons in this sample are typical. Zircons in this sample, transparent with light yellow color, generally have rhythm zoning (Fig. 3). A total of 11 spots were analyzed (Table 1), including 4 cores from 4 zircon grains. It is similar to sample 04BD-26 that two core spots (D3.1 and D11.1) give old $^{206}Pb/^{238}U$ ages of ca. 880 and ca. 950 Ma, respectively. Spot D9.1 and D9.2 were analyzed from the core and rim of one zircon, respectively, and give Mesoproterozoic ages. It suggests that this zircon is inherited. The other core spot (D8.1) gives a concordant age of 692 Ma, but with very high ^{238}U and low Th/U value (0.08). It might be due to an overprinting metamorphic event. One spot analysis (D6.1) shows a concordant age of ca. 900 Ma. The remaining five spots yield a weighted mean $^{206}Pb/^{238}U$ age of 824 ± 13 Ma (Fig. 4, 95% confidence, MSWD = 0.23) that is interpreted as the crystallization age of the Dongma pluton. This age overlaps with that of the Bendong pluton. The Dongma pluton has previously been regarded as a southern extension of the Bendong pluton (Ge et al., 2001a). Combining 27 analyses from the two plutons yields a precise weighted mean $^{206}Pb/^{238}U$ age of 822.8 ± 3.7 Ma (95% confidence, MSWD = 0.80).

4.4. Sample SF-35, Sanfang granite

Sample SF-35, coarse-grained biotite granite with sericitization, is composed of plagioclase ($An_{27–28}$), quartz, K-feldspar, biotite and a minor muscovite and tourmaline. Zircons in this sample are pale yellow to transparent, euhedral, and have rhythmic zoning (Fig. 3), suggesting magmatic origin. A total of 18 spots from 15 zircons were analyzed. Two core spots yield

Table 1
Laser ablation ICP-MS U-Th-Pb analyses for the igneous rocks from Northern Guangxi, South China

Spot	Concentrations (ppm)			Th/U	U–Th–Pb isotopic ratios								Ages (Ma)							
	Pb_{rad}	^{232}Th	^{238}U		207/206	1σ	206/238	1σ	207/235	1σ	208/232	1σ	207/206	1σ	206/238	1σ	207/235	1σ	208/232	1σ
CG-25, Zhaigun																				
C5.01	31.2	81	169	0.48	0.0678	0.0009	0.1386	0.0007	1.2956	0.0120	0.0438	0.0003	863	11	836	4	844	5	867	6
C5.03	81.3	413	381	1.08	0.0723	0.0009	0.1377	0.0007	1.3720	0.0124	0.0436	0.0002	993	10	831	4	877	5	862	4
C5.06	36.0	114	190	0.60	0.0677	0.0010	0.1388	0.0008	1.2965	0.0153	0.0430	0.0004	861	15	838	4	844	7	852	7
C5.08	5.8	29	28	1.05	0.0664	0.0022	0.1355	0.0026	1.2402	0.0331	0.0431	0.0014	819	71	819	15	819	15	853	26
C5.09	19.4	47	106	0.44	0.0704	0.0019	0.1370	0.0013	1.3305	0.0333	0.0482	0.0009	941	36	828	7	859	14	951	17
C5.10	111.1	286	605	0.47	0.0701	0.0008	0.1391	0.0006	1.3458	0.0095	0.0426	0.0002	932	8	840	4	866	4	843	5
C5.11	96.5	354	493	0.72	0.0697	0.0012	0.1385	0.0009	1.3318	0.0193	0.0440	0.0004	920	20	836	5	860	8	871	8
C5.12	48.4	177	246	0.72	0.0666	0.0010	0.1391	0.0007	1.2788	0.0142	0.0445	0.0003	827	14	840	4	836	6	880	6
C5.13	27.0	91	139	0.65	0.0691	0.0022	0.1383	0.0015	1.3176	0.0395	0.0465	0.0009	901	44	835	8	853	17	919	17
C5.14	53.0	114	294	0.39	0.0680	0.0008	0.1381	0.0007	1.2954	0.0104	0.0475	0.0003	869	9	834	4	844	5	938	6
C5.17	26.8	132	127	1.03	0.0681	0.0012	0.1375	0.0009	1.2912	0.0202	0.0451	0.0004	871	22	831	5	842	9	892	7
C5.18	20.2	54	109	0.50	0.0670	0.0024	0.1382	0.0017	1.2771	0.0446	0.0477	0.0011	838	52	834	10	836	20	942	22
C5.21	56.3	220	284	0.78	0.0665	0.0008	0.1390	0.0007	1.2756	0.0104	0.0438	0.0002	823	9	839	4	835	5	865	5
C5.23	57.8	192	295	0.65	0.0743	0.0021	0.1379	0.0014	1.4134	0.0371	0.0496	0.0008	1050	37	833	8	895	16	979	16
C5.24	51.4	184	264	0.70	0.0693	0.0011	0.1387	0.0008	1.3250	0.0175	0.0442	0.0004	907	18	837	5	857	8	873	7
04BD-26, Bendong																				
B1.2	38.6	71	235	0.30	0.0665	0.0015	0.1353	0.0016	1.2403	0.0279	0.0468	0.0010	821	47	818	9	819	13	925	20
B2.1	29.1	67	187	0.36	0.0666	0.0016	0.1365	0.0017	1.2531	0.0302	0.0431	0.0010	825	50	825	9	825	14	853	19
B3.1	80.8	95	527	0.18	0.0659	0.0012	0.1364	0.0015	1.2406	0.0222	0.0425	0.0007	804	37	825	9	819	10	841	13
B5.1	53.7	87	368	0.24	0.0662	0.0012	0.1336	0.0015	1.2190	0.0226	0.0452	0.0008	812	39	808	9	809	10	894	15
B6.1	43.0	83	276	0.30	0.0665	0.0015	0.1366	0.0016	1.2521	0.0276	0.0452	0.0009	822	46	825	9	824	12	893	17
B7.1	43.4	86	292	0.29	0.0663	0.0017	0.1350	0.0017	1.2339	0.0311	0.0422	0.0010	815	53	817	9	816	14	836	19
B8.1	59.2	89	409	0.22	0.0661	0.0016	0.1335	0.0016	1.2160	0.0290	0.0429	0.0010	808	50	808	9	808	13	849	19
B9.1	148.1	109	997	0.11	0.0665	0.0012	0.1360	0.0015	1.2461	0.0219	0.0456	0.0009	821	36	822	9	822	10	901	17
B11.1	26.5	87	161	0.54	0.0661	0.0014	0.1373	0.0016	1.2508	0.0270	0.0423	0.0006	808	45	830	9	824	12	836	12
B12.1	57.4	91	382	0.24	0.0664	0.0011	0.1351	0.0015	1.2375	0.0204	0.0417	0.0007	820	34	817	8	818	9	825	13
B13.1	76.6	61	432	0.14	0.0665	0.0018	0.1357	0.0017	1.2430	0.0333	0.0426	0.0010	821	56	820	10	820	15	843	19
B14.1	36.9	114	233	0.49	0.0663	0.0013	0.1348	0.0016	1.2325	0.0247	0.0401	0.0006	816	42	815	9	816	11	794	12
B15.1	37.2	56	247	0.23	0.0663	0.0013	0.1350	0.0015	1.2350	0.0240	0.0421	0.0008	817	41	817	9	817	11	834	15
B16.1	82.0	78	545	0.14	0.0666	0.0015	0.1363	0.0016	1.2503	0.0270	0.0467	0.0010	824	45	824	9	824	12	923	20
B17.1	78.9	224	474	0.47	0.0667	0.0015	0.1353	0.0016	1.2446	0.0274	0.0403	0.0006	829	46	818	9	821	12	799	12
B20.1	49.1	84	308	0.27	0.0647	0.0016	0.1363	0.0016	1.2167	0.0285	0.0450	0.0009	766	50	824	9	808	13	889	17
B21.1	52.2	142	311	0.46	0.0668	0.0018	0.1377	0.0017	1.2684	0.0338	0.0391	0.0008	833	56	831	10	832	15	775	15
B1.1[a]	20.8	56	118	0.48	0.0748	0.0022	0.1782	0.0023	1.8370	0.0520	0.0487	0.0012	1062	57	1057	13	1059	19	961	23
B4.1[a]	11.8	50	71	0.70	0.0664	0.0020	0.1355	0.0017	1.2396	0.0368	0.0454	0.0008	818	62	819	10	819	17	897	15
B6.2[a]	11.9	46	71	0.65	0.0666	0.0024	0.1368	0.0019	1.2559	0.0434	0.0435	0.0009	824	72	827	11	826	20	860	18
B10.1[a]	69.0	71	460	0.15	0.0646	0.0011	0.1376	0.0015	1.2250	0.0210	0.0428	0.0008	760	36	831	9	812	10	847	15
B18.1[a]	47.6	51	243	0.21	0.0683	0.0015	0.1530	0.0018	1.4409	0.0303	0.0487	0.0011	878	44	918	10	906	13	961	22
B19.1[a]	61.7	94	378	0.25	0.0674	0.0016	0.1406	0.0016	1.3072	0.0294	0.0470	0.0010	851	47	848	9	849	13	928	18
B22.1[a]	24.9	77	142	0.54	0.0669	0.0019	0.1386	0.0017	1.2786	0.0358	0.0416	0.0008	835	59	837	10	836	16	823	15
B23.1[a]	21.7	41	125	0.33	0.0698	0.0026	0.1552	0.0022	1.4946	0.0552	0.0422	0.0013	923	76	930	12	928	22	835	26

04DM-22, Dongma																			
D1.1	23.5	88	140	0.63	0.0821	0.0040	0.1367	0.0025	1.5473	0.0745	0.0415	0.0014	1248	93	826	14	949	30	823	27
D2.1	39.6	173	229	0.76	0.0796	0.0031	0.1358	0.0022	1.4897	0.0571	0.0430	0.0010	1187	75	821	13	926	23	851	19
D5.1	30.3	73	191	0.38	0.0790	0.0030	0.1364	0.0022	1.4850	0.0557	0.0391	0.0013	1172	73	824	13	924	23	776	24
D7.1	71.3	59	317	0.19	0.2216	0.0199	0.1368	0.0056	4.1815	0.3480	0.3320	0.0218	2993	138	827	31	1670	68	5795	330
D6.1	43.8	108	250	0.43	0.0688	0.0033	0.1506	0.0027	1.4292	0.0667	0.0374	0.0014	893	95	904	15	901	28	742	27
D9.2	342.3	732	952	0.77	0.0997	0.0016	0.2743	0.0036	3.7713	0.0651	0.0750	0.0009	1619	29	1562	18	1587	14	1462	17
D10.1	38.6	278	197	1.41	0.0719	0.0039	0.1365	0.0026	1.3532	0.0726	0.0342	0.0009	983	108	825	15	869	31	679	17
D3.1[a]	74.6	104	464	0.23	0.0690	0.0021	0.1454	0.0021	1.3836	0.0430	0.0439	0.0013	900	63	875	12	882	18	868	26
D8.1[a]	120.2	75	974	0.08	0.0625	0.0058	0.1132	0.0030	0.9759	0.0880	0.0441	0.0059	691	185	692	17	692	45	872	114
D9.1[a]	61.0	140	132	1.06	0.1160	0.0031	0.3321	0.0051	5.3120	0.1412	0.0888	0.0016	1895	47	1849	25	1871	23	1720	29
D11.1[a]	64.7	65	356	0.18	0.0710	0.0078	0.1582	0.0051	1.5485	0.1653	0.0545	0.0066	957	209	947	28	950	66	1073	126
SF-35, Sanfang																			
S1.2	69.2	73	460	0.16	0.0660	0.0021	0.1324	0.0019	1.2055	0.0382	0.0393	0.0014	807	66	802	11	803	18	779	27
S2.1	81.3	292	482	0.60	0.0662	0.0017	0.1322	0.0018	1.2071	0.0310	0.0373	0.0006	813	53	801	10	804	14	741	12
S6.2	101.0	65	666	0.10	0.0661	0.0014	0.1341	0.0017	1.2227	0.0261	0.0405	0.0012	810	43	811	10	811	12	803	22
S7.1	73.4	67	482	0.14	0.0643	0.0015	0.1333	0.0017	1.1820	0.0272	0.0400	0.0011	752	47	807	10	792	13	793	21
S8.1	51.6	59	335	0.18	0.0658	0.0017	0.1334	0.0018	1.2103	0.0321	0.0376	0.0011	800	55	807	10	805	15	746	21
S9.1	120.2	155	770	0.20	0.0661	0.0021	0.1337	0.0019	1.2183	0.0388	0.0379	0.0013	809	66	809	11	809	18	752	24
S10.1	70.4	199	426	0.47	0.0660	0.0019	0.1320	0.0018	1.2008	0.0339	0.0369	0.0008	805	58	800	10	801	16	732	15
S11.1	69.3	120	439	0.27	0.0647	0.0017	0.1319	0.0018	1.1767	0.0314	0.0401	0.0009	765	55	799	10	790	15	794	18
S13.2	42.6	16	289	0.05	0.0646	0.0019	0.1309	0.0018	1.1652	0.0339	0.0399	0.0022	761	61	793	10	784	16	790	42
S14.1	47.5	114	289	0.39	0.0659	0.0021	0.1326	0.0019	1.2048	0.0380	0.0383	0.0009	803	65	803	11	803	18	759	18
S15.1	64.3	54	420	0.13	0.0656	0.0019	0.1332	0.0019	1.2056	0.0339	0.0343	0.0013	795	58	806	11	803	16	681	25
S16.1	70.3	84	457	0.18	0.0650	0.0015	0.1316	0.0017	1.1795	0.0270	0.0370	0.0009	775	47	797	10	791	13	734	17
S17.1	20.4	54	124	0.43	0.0657	0.0041	0.1316	0.0027	1.1921	0.0731	0.0362	0.0017	798	126	797	15	797	34	719	32
S3.2[a]	42.5	133	255	0.52	0.0658	0.0020	0.1326	0.0019	1.2026	0.0365	0.0392	0.0008	798	63	803	11	802	17	777	15
S7.2[a]	28.9	58	183	0.32	0.0669	0.0027	0.1315	0.0021	1.2127	0.0487	0.0376	0.0013	835	83	796	12	806	22	746	25
S5.1[a]	55.1	17	325	0.05	0.0700	0.0032	0.1499	0.0026	1.4468	0.0657	0.0889	0.0061	928	92	900	14	909	27	1722	114
S6.1[a]	63.1	66	400	0.17	0.0668	0.0016	0.1376	0.0018	1.2676	0.0306	0.0371	0.0010	832	49	831	10	831	14	735	20
S13.1[a]	15.4	78	67	1.17	0.0696	0.0049	0.1519	0.0033	1.4568	0.0998	0.0469	0.0014	916	138	912	19	913	41	926	27
TB-28, Tianpeng																			
T1.1	46.4	106	328	0.32	0.0623	0.0035	0.1310	0.0025	1.1215	0.0609	0.0341	0.0017	684	114	793	14	764	29	677	33
T2.1	20.2	123	117	1.04	0.0660	0.0043	0.1333	0.0029	1.2103	0.0769	0.0391	0.0012	808	131	806	16	805	35	776	24
T3.1	41.8	72	307	0.23	0.0651	0.0038	0.1287	0.0026	1.1530	0.0662	0.0319	0.0021	779	119	780	15	779	31	635	41
T4.1	29.7	67	209	0.32	0.0654	0.0034	0.1293	0.0024	1.1630	0.0596	0.0398	0.0018	787	106	784	14	783	28	789	34
T6.1	50.4	204	343	0.59	0.0648	0.0028	0.1261	0.0021	1.1235	0.0472	0.0358	0.0010	767	88	766	12	765	23	711	19
T7.1	46.8	122	314	0.39	0.0655	0.0031	0.1327	0.0024	1.1949	0.0557	0.0422	0.0015	789	97	803	13	798	26	836	29
T8.1	60.5	338	348	0.97	0.0672	0.0038	0.1384	0.0028	1.2804	0.0709	0.0373	0.0011	845	114	836	16	837	32	740	22
T10.1	52.9	79	379	0.21	0.0657	0.0031	0.1312	0.0023	1.1856	0.0550	0.0369	0.0019	796	96	795	13	794	26	732	36
T10.2	113.7	81.1	860	0.09	0.0649	0.0024	0.1281	0.0020	1.1439	0.0414	0.0359	0.0020	770	75	777	11	774	20	713	39.5
T11.2	60.1	79	433	0.18	0.0649	0.0034	0.1307	0.0024	1.1691	0.0600	0.0412	0.0023	772	107	792	14	786	28	817	45

Table 1 (*Continued*)

Spot	Concentrations (ppm)			Th/U	U–Th–Pb isotopic ratios								Ages (Ma)							
	Pb_{rad}	^{232}Th	^{238}U		207/206	1σ	206/238	1σ	207/235	1σ	208/232	1σ	207/206	1σ	206/238	1σ	207/235	1σ	208/232	1σ
T12.1	124.9	69	913	0.08	0.0653	0.0060	0.1303	0.0036	1.1720	0.1050	0.0725	0.0085	784	182	790	21	788	49	1415	160
T13.1	78.6	113	563	0.20	0.0638	0.0037	0.1317	0.0026	1.1590	0.0655	0.0348	0.0022	737	118	798	15	782	31	691	43
T15.2	46.2	66	318	0.21	0.0665	0.0029	0.1359	0.0023	1.2458	0.0526	0.0388	0.0017	822	87	821	13	822	24	769	34
T16.1	51.6	97	310	0.31	0.0668	0.0008	0.1320	0.0006	1.2156	0.0080	0.0412	0.0003	830	23	800	3	808	4	816	5
T17.1	32.1	82	190	0.43	0.0668	0.0012	0.1283	0.0008	1.1818	0.0188	0.0426	0.0005	832	38	778	5	792	9	844	10
T4.2[a]	48.1	161	242	0.67	0.0734	0.0032	0.1697	0.0030	1.7130	0.0724	0.0429	0.0013	1024	85	1011	16	1013	27	850	25
T9.1[a]	92.3	71	433	0.16	0.0968	0.0019	0.1949	0.0027	2.5971	0.0510	0.0699	0.0016	1564	36	1148	14	1300	14	1367	31
T10.3[a]	73.6	116	402	0.29	0.0738	0.0023	0.1660	0.0025	1.6870	0.0512	0.0523	0.0015	1036	60	990	14	1004	19	1030	28
T11.1[a]	101.7	120	465	0.26	0.0798	0.0018	0.1956	0.0027	2.1485	0.0482	0.0756	0.0015	1191	43	1152	15	1165	16	1473	28
T12.2[a]	71.2	94	321	0.29	0.0782	0.0024	0.2020	0.0031	2.1771	0.0673	0.0533	0.0017	1152	61	1186	17	1174	22	1050	32
T14.2[a]	130.4	110	1026	0.11	0.0642	0.0017	0.1221	0.0017	1.0802	0.0287	0.0379	0.0013	747	55	743	10	744	14	752	25
T15.1[a]	57.7	155	374	0.41	0.0663	0.0019	0.1373	0.0020	1.2536	0.0359	0.0384	0.0008	814	59	829	11	825	16	761	16
04HJW-7, Hejiawan																				
H1.1	47.5	216	272	0.79	0.0694	0.0022	0.1342	0.0017	1.2853	0.0390	0.0387	0.0007	912	63	812	10	839	17	768	13
H2.1	58.1	117	371	0.32	0.0662	0.0019	0.1349	0.0017	1.2312	0.0348	0.0423	0.0010	812	59	816	10	815	16	837	19
H3.1	62.9	121	403	0.30	0.0708	0.0016	0.1340	0.0016	1.3077	0.0295	0.0445	0.0008	951	46	811	9	849	13	880	16
H4.1	37.3	86	235	0.36	0.0705	0.0017	0.1339	0.0016	1.3016	0.0309	0.0438	0.0008	942	49	810	9	846	14	867	16
H5.1	95.7	143	624	0.23	0.0719	0.0019	0.1339	0.0016	1.3282	0.0339	0.0471	0.0011	984	52	810	9	858	15	931	22
H7.1	45.0	116	277	0.42	0.0774	0.0019	0.1342	0.0016	1.4322	0.0340	0.0456	0.0008	1132	48	812	9	903	14	901	16
H8.1	68.7	175	432	0.40	0.0681	0.0019	0.1345	0.0017	1.2628	0.0350	0.0411	0.0009	872	58	814	10	829	16	813	17
H9.1	87.3	152	570	0.27	0.0704	0.0013	0.1342	0.0015	1.3036	0.0239	0.0410	0.0007	941	38	812	8	847	11	812	13
H10.1	94.6	155	680	0.23	0.0703	0.0014	0.1228	0.0014	1.1900	0.0230	0.0397	0.0007	936	40	747	8	796	11	787	14
H11.1	70.3	291	447	0.65	0.0684	0.0019	0.1255	0.0015	1.1843	0.0315	0.0384	0.0007	881	55	762	9	793	15	761	13
H12.1	49.9	143	308	0.46	0.0717	0.0018	0.1339	0.0016	1.3240	0.0323	0.0439	0.0008	978	50	810	9	856	14	868	15
H14.1	64.0	97	433	0.22	0.0901	0.0025	0.1230	0.0016	1.5276	0.0402	0.0696	0.0016	1428	51	748	9	942	16	1360	30
H15.1	57.2	108	374	0.29	0.0688	0.0020	0.1336	0.0017	1.2677	0.0362	0.0429	0.0011	894	59	808	10	831	16	848	21
H16.1	92.2	94	662	0.14	0.0747	0.0017	0.1241	0.0015	1.2784	0.0277	0.0565	0.0013	1062	44	754	8	836	12	1111	25
H17.1	64.5	133	418	0.32	0.0662	0.0015	0.1341	0.0015	1.2247	0.0266	0.0434	0.0008	814	46	811	9	812	12	859	15
H18.1	44.8	210	277	0.76	0.0713	0.0034	0.1244	0.0020	1.2225	0.0565	0.0417	0.0011	966	94	756	12	811	26	826	21
H19.1	63.6	105	413	0.25	0.0734	0.0018	0.1343	0.0016	1.3598	0.0320	0.0491	0.0011	1026	48	812	9	872	14	970	21
H20.1	81.0	194	543	0.36	0.0808	0.0019	0.1238	0.0015	1.3781	0.0309	0.0505	0.0009	1216	45	752	8	880	13	996	18
H21.1	60.8	123	385	0.32	0.0761	0.0015	0.1338	0.0015	1.4029	0.0262	0.0537	0.0009	1097	37	809	9	890	11	1058	16
H22.1	59.6	213	385	0.55	0.0664	0.0020	0.1347	0.0017	1.2330	0.0354	0.0256	0.0006	819	60	815	10	816	16	510	12
H13.1[a]	144.7	67	923	0.07	0.0681	0.0011	0.1445	0.0016	1.3579	0.0214	0.0597	0.0013	873	33	870	9	871	9	1173	24

[a] Analyzed from zircon cores.

early Neoproterozoic ages (Table 1, $^{206}Pb/^{238}U$ ages of 900 ± 14 Ma for spot S5.1 and 912 ± 19 Ma for S13.1). The remaining 16 spots yield a precise weighted mean $^{206}Pb/^{238}U$ age of 804.3 ± 5.2 Ma (Fig. 4, 95% confidence, MSWD = 0.74). We detected that a concordant age of spot S6.1 (ca. 830 Ma, Table 1) is relatively old. It might be resulted from the lead loss or analytical error because this analysis result was got from the core spot, whereas the rim analysis from the same zircon yielded a very concordant age of ca. 810 Ma similar to the weighted mean ages of this sample. Li (1999) reported a SHRIMP U-Pb age of 826 ± 10 Ma for the Sanfang pluton. But the age was based on only five spot analyses and indistinguishable with that of the Bendong pluton. The age of 804.3 ± 5.2 Ma is clearly younger than that of the Bendong pluton, in agreement with the field relationships. In light of our new data, we believe that an age of 804.3 ± 5.2 Ma may better reflect the crystallization age of the Sanfang pluton.

4.5. Sample TB-28, Tianpeng granite

Sample TB-28 is a coarse-grained granite, composed of plagioclase, perthite, and quartz with lesser amounts of biotite and muscovite. Euhedral zircons in this sample appear pale yellow or brown yellow, transparent, and have rhythmic zoning (Fig. 3). A total of 22 spots (15 rims and 7 cores) from 16 grains were analyzed (Table 1). Except for analysis T9.1 ($^{207}Pb/^{206}Pb$ age of 1148 ± 14 Ma), all analyses plotted on the concordia (Fig. 4). Four core analyses (spots T4.2, T10.3, T11.1 and T12.2) reveal Mesoproterozoic ages ($^{207}Pb/^{206}Pb$ age of 1024 ± 85 Ma, 1036 ± 60 Ma, 1191 ± 43 Ma and 1152 ± 61 Ma, respectively). One core analysis (T14.2) gives a younger age near 750 Ma, due to high ^{238}U contents and low Th/U ratios (0.11), this may imply a metamorphic origin. The remaining 16 spots of the sample yield a weighted mean $^{206}Pb/^{238}U$ age of 794.2 ± 8.1 Ma (95% confidence, MSWD = 3.1), which represents the crystallization age of the Tianpeng granite.

4.6. Sample 04HJW-7, Hejiawan diabase

Sample 04HJW-7, a diabase, is composed of plagioclase and clinopyroxene that was altered and replaced by tremolite and zoisite. Transparent, colorless zircon grains in this sample are very small (about 50–60 μm in length and 25–30 μm in width). The rhythm zoning of this sample is not very clear, and some zircons have a narrow white rim (Fig. 3). A total of 21 zircons were analyzed (Table 1). Most data of the analyses are shifted to the right of the concordia due to the analytical uncertainty of the ^{207}Pb (Fig. 4). One core spot (H13.1, Fig. 3) gives an inherited concordant age of ca. 870 Ma, with Th/U ratio of 0.07, probably suggesting a metamorphic origin. Of the remaining 20 rim analyses, 14 spots give a weighted mean $^{206}Pb/^{238}U$ age of 811.5 ± 4.8 Ma (95% confidence, MSWD = 0.047), whereas 6 analyses yield an age of 752.7 ± 7.1 Ma (95% confidence, MSWD = 0.43). Compared with the former 14 analyses, the $^{207}Pb/^{206}Pb$, $^{207}Pb/^{235}U$, $^{206}Pb/^{238}U$ and $^{208}Pb/^{232}Th$ ages in each spot of the latter 6 analyses are generally inconsistent with each other. Moreover, the weighted age of 752.7 ± 7.1 Ma is consistent with a later magmatic event at the western part of the Jiangnan orogen, such as the Longsheng mafic-ultramafic rocks (ca. 761 Ma; Ge et al., 2000) from Northern Guangxi and the mafic rocks (ca. 755 Ma, our unpublished data) from Qianyang of Hunan Province. And it is very similar to a metamorphic age (ca. 750 Ma) of the sample TB-28. So, the 752.7 ± 7.1 Ma age of 04HJW-7 may be caused by the overgrowth of zircon due to the fluid related to the thermal event, as revealed by the narrow white rims from some grains of this sample in Fig. 3. The age of 811.5 ± 4.8 Ma should represent the crystallization age of the Hejiawan layered diabase, and it is slightly younger than that of the Yangmeiao mafic-ultramafic rocks reported by Li et al. (1999).

5. Geochemistry

The geochemical characteristics of the Neoproterozoic mafic-ultramafic rocks in the study area have been discussed by Zhou et al. (2004) in detail. These rocks display arc-like geochemical signatures and are thought to be the products of magmatism of convergent plate boundary rather than derived from mantle plume (Zhou et al., 2004). In this work, we dominantly discuss the geochemistry of the granitoids in the Baotan, Sanfang and Yuanbaoshan areas.

The major, trace element and isotopic data of the granitoids are listed in Table 2. According to the TAS diagram (not shown here), these samples are divided into two main rock types: granodiorites and granites. The granodiorites show variable major oxides contents with SiO_2 from 59.21 to 76.94%, and they have higher TiO_2, MnO, MgO, CaO, Mg#, Ni, Cr, V and Sc contents and CaO/Na_2O ratios than the granites. All the samples are strongly peraluminous with high ACNK values ranging from 1.10 to 1.87 and normative corundum of 1.53–3.85%, exhibiting typical features of S-type granites (Chappell and White, 1974). Most of the samples have high K_2O/Na_2O ratios (1.31–2.26). The granodi-

Table 2
Major, trace element and Sr-Nd isotopic data for the Neoproterozoic granitoids from Northern Guangxi, South China

Location no. sample	Bendong		Mengdong	Dazhai	Dongma		Longyou	Zhaigun	Yuanbaoshan		Pingying		Tianpeng	Sanfang
	1[a]	2[a]	3[a]	4[a]	5[a]	6[a]	7[a]	8[a]	9[b]	10[b]	11[b]	12[b]	13[b]	14[b]
	04BD-26	BD-37	MD-5	DZ-23	04DM-21	04DM-22	LY-21	CG-26	04YBS-36	04YBS-40	PY-7	PY-13	TB-28	SF-35
Major elements (wt%)														
SiO_2	70.28	70.82	69.52	65.78	59.21	66.55	65.00	66.58	72.53	74.71	72.26	76.70	75.66	76.94
TiO_2	0.47	0.26	0.35	0.55	0.54	0.46	0.54	0.54	0.26	0.15	0.05	0.07	0.07	0.20
Al_2O_3	13.20	14.79	14.86	15.46	13.76	15.49	14.74	15.23	14.29	13.30	13.10	13.09	12.82	11.79
Fe_2O_3	4.85[c]	0.69	1.30	1.06	7.13[c]	4.73[c]	1.27	1.56	2.67[c]	2.02[c]	0.56	0.81	0.37	0.69
FeO		1.97	2.04	3.73			3.82	3.07			0.86	0.38	1.10	1.41
MnO	0.12	0.06	0.08	0.09	0.14	0.08	0.09	0.10	0.06	0.05	0.03	0.04	0.03	0.05
MgO	2.11	1.48	1.80	2.87	8.92	3.37	3.48	2.76	0.71	0.37	0.26	0.26	0.20	0.54
CaO	2.29	1.58	1.88	2.92	1.93	2.73	3.15	3.25	0.62	0.68	0.30	0.27	0.50	1.14
Na_2O	2.03	2.59	2.43	2.32	1.05	2.75	2.18	2.46	2.09	2.58	2.80	2.59	3.08	2.18
K_2O	2.65	4.03	4.20	3.14	1.97	1.94	3.21	3.28	4.72	4.81	5.16	5.12	5.26	4.07
P_2O_5	0.18	0.24	0.18	0.26	0.10	0.13	0.17	0.17	0.13	0.12	0.23	0.15	0.18	0.16
LOI[d]	1.62	1.26	1.43	1.60	5.06	1.66	1.73	1.41	1.64	0.81	0.82	0.95	0.94	0.81
Total	99.80	99.77	100.07	99.78	99.81	99.89	99.38	100.41	99.72	99.60	100.43	100.43	100.21	99.98
Mg#[e]	46.3	50.5	50.0	52.2	71.2	58.5	55.6	52.4	34.5	26.6	25.4	29.5	19.9	32.2
ACNK[f]	1.27	1.29	1.24	1.23	1.87	1.34	1.15	1.13	1.48	1.24	1.22	1.27	1.10	1.17
C[g]		3.85	3.31	3.60			2.35	2.09			2.97	3.12	1.53	2.07
CaO/Na_2O	1.13	0.61	0.77	1.26	1.84	0.99	1.44	1.32	0.30	0.26	0.11	0.10	0.16	0.52
K_2O/Na_2O	1.31	1.56	1.73	1.35	1.88	0.71	1.47	1.33	2.26	1.86	1.84	1.98	1.71	1.87
Trace elments (ppm)														
Rb	103.5	191	191	131	111.1	83.52	143	141	208.1	336.1	404	459	428	223
Sr	209.3	150	200	152	124.5	217.2	164	162	63.20	91.27	15	14	13	56
Ba	423.8	624	715	500	379.6	383.5	507	638	277.1	222.1	291	301	74	158
Nb	11.96	9.55	12.14	12.16	7.30	9.87	11.15	11.87	9.55	9.11	12.87	16.62	12.70	8.64
Ta	1.27	1.39	1.27	1.15	0.55	0.90	0.93	1.16	1.06	1.70	2.98	4.00	2.94	1.37
Zr	254.3	104.7	163.8	221.0	181.6	200.0	185.0	213.3	156.4	100.5	61.70	67.39	82.11	124.1
Hf	6.77	2.83	4.62	5.05	4.75	5.80	4.26	5.36	4.83	3.19	2.51	2.79	3.11	3.75
Pb	22.22	29	40	22	16.45	26	13	35	30.23	25.98	33	29	29	30
Th	18.11	8.67	12.11	10.10	7.50	12.73	9.32	11.66	17.20	15.48	8.94	11.98	9.84	13.21
U	3.52	7.79	3.12	2.18	1.52	2.27	2.14	2.20	2.75	8.89	3.91	7.06	8.78	2.53

Cr	114.2	147.1	65.67	151.6	1309	343.1	176.0	89.09	44.20	18.66	24.09	63.26	34.17	45.13
Co	12.82	4	7	12	35.82	15.8	11.00	12	6.31	2.54	-	6	-	5
Ni	23.7	26	26	54	205.5	59.6	68	39	12.27	20.99	12	11	10	12
Y	38.09	24.66	32.19	27	42.62	22.13	27.95	29.93	29.34	36.96	25.31	26.92	26.30	42.10
V	68.52	35	44	86	104.8	42.75	105	66	29.58	15.52	8	5	4	23
Sc	10.82	9.70	11.48	15.79	15.70	10.50	16.86	14.75	4.99	4.22	4.20	4.40	4.19	5.64
La	35.05	28.10	38.71	38.06	29.07	32.59	37.96	38.57	30.30	16.69	8.70	8.16	11.43	27.78
Ce	60.36	54.24	78.41	77.43	36.22	53.67	73.19	75.67	50.33	30.46	18.67	17.76	22.07	52.76
Pr	6.81	6.22	9.07	8.94	5.45	6.42	8.43	8.65	6.69	3.58	2.71	2.65	2.97	6.27
Nd	29.86	24.36	35.81	34.97	24.77	25.99	33.78	34.38	26.20	14.67	8.26	8.07	9.23	22.83
Sm	7.93	5.01	7.29	6.91	6.41	5.48	6.60	6.76	6.70	4.27	2.58	2.55	2.74	5.24
Eu	1.07	0.94	1.25	1.22	1.70	1.16	1.21	1.21	0.65	0.33	0.07	0.10	0.12	0.51
Gd	5.61	4.86	6.80	6.48	4.73	3.95	5.95	6.12	4.97	3.49	2.96	3.04	3.16	5.76
Tb	0.99	0.74	0.98	0.93	0.89	0.64	0.85	0.88	0.94	0.79	0.64	0.67	0.66	1.00
Dy	6.12	4.32	5.79	5.47	6.40	3.62	4.93	5.27	5.97	5.53	4.36	4.67	4.48	6.77
Ho	1.36	0.89	1.19	1.15	1.39	0.82	1.02	1.10	1.30	1.33	0.85	0.94	0.87	1.48
Er	3.40	2.27	3.03	2.95	3.53	2.14	2.60	2.85	3.54	3.40	2.24	2.53	2.29	3.94
Tm	0.57	0.35	0.47	0.47	0.56	0.35	0.41	0.44	0.57	0.55	0.39	0.43	0.39	0.61
Yb	3.58	2.29	3.08	3.11	3.23	2.07	2.66	2.94	3.23	3.62	2.66	3.08	2.68	4.01
Lu	0.52	0.34	0.46	0.47	0.56	0.36	0.39	0.44	0.51	0.56	0.36	0.42	0.36	0.55
Isotope														
$^{87}Rb/^{86}Sr$			2.819				2.575	2.583				111.5	102.7	
$^{87}Sr/^{86}Sr$			0.739727 ± 16				0.741424 ± 25	0.740745 ± 26				2.092057 ± 41	2.112355 ± 39	
I_{sr}[h]			0.707				0.711	0.710				0.818	0.939	
$^{147}Sm/^{144}Nd$			0.1158				0.1181	0.1152				0.1905	0.1617	
$^{143}Nd/^{144}Nd$			0.512033 ± 5				0.511938 ± 5	0.511943 ± 4				0.512391 ± 10	0.512304 ± 9	
T(2DM) (Ma)[h]			1759				1929	1896				1813	1712	
ε(Nd)[h]			−3.27				−5.37	−4.86				−4.19	−2.94	

[a] Granodiorite.
[b] Granite.
[c] Fe_2O_3 as total iron.
[d] LOI, loss on ignition.
[e] $Mg^{\#} = 100*Mg^{2+}/(Fe^{2+} + Mg^{2+})$, Fe^{2+} is calculated from total FeO.
[f] ACNK, molecular ratio of $Al_2O_3/(CaO + Na_2O + K_2O)$.
[g] Normative corundum.
[h] Calculated based on the age results of this work.

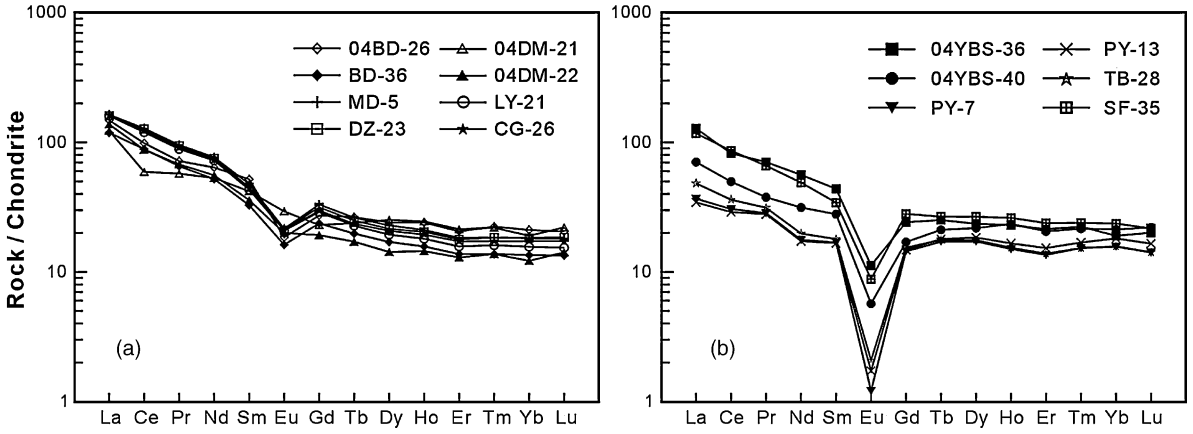

Fig. 5. Chondrite-normalized REE patterns for the Neoproterozoic igneous rocks from Northern Guangxi. (a) Granodiorites; (b) granites.

orites have relatively high REE contents and show similar REE patterns with moderate Eu negative anomaly (Fig. 5a), whereas the granites have flat REE patterns with variable LREE abundances and pronounced Eu negative anomaly (Fig. 5b), implying the fractionation of the feldspar.

The initial ($^{87}Sr/^{86}Sr$) (I_{Sr}) ratios of the granodiorites are moderate (0.707∼0.711). Whereas, calculated I_{Sr} values of granites are very high ranging from 0.818 to 0.939, suggesting that their Rb–Sr isotopic system might be disturbed by the late tectono-thermal events as revealed by the high Rb/Sr ratios of these rocks. Average ε_{Nd} (T) of these granitoids is −4.13, in line with the Neoproterozoic strongly peraluminous granites in Xiuning and Xucun plutons in the eastern part of the Jiangnan orogen (Xu and Zhou, 1992; Li XH et al., 2003).

6. Discussion

6.1. Petrogenesis

The generation of S-type granites is generally interpreted in terms of partial melting of metasedimentary rocks in the source region (Clemens, 2003). The Nd model ages of the granitoids from Northern Guangxi range from 1.71 to 1.93 Ga, which are comparable with those of the Mesoproterozoic sedimentary rocks (1.80–1.91 Ga) of the Sibao Group (Li et al., 1991; Chen and Jahn, 1998). In addition, our new LA-ICP-MS geochronological data also give a set of Mesoproterozoic age of ca. 1.9–1.0 Ga from some zircon cores and one single relict zircon, falling within the age range of the Sibao Group (ca. 1.85–1.0 Ga; Li, 1999). The isotopic and geochronological evidence implies that the source rocks of the S-type granites in Northern Guangxi may be the Mesoproterozoic strata or its equivalents. Then, what was the heat source for the partial melting of the metasediments in Northern Guangxi? It was proposed that a ca. 820 Ma mantle plume or superplume centered beneath South China triggered the breakup of the Rodinia supercontinent and caused the partial melting of the crustal materials to generate these S-type granites along the Jiangnan orogen (Li XH et al., 2003; Li et al., 1999; Li ZX et al., 2003). However, it is commonly believed that both scale and intensity of a mantle plume activity is inconceivable large, and the generated rock types are confined to special rock associations (e.g., Condie, 2001; Bryan et al., 2002). S-type granites related with the magmatism of mantle plume have not been reported so far. Many geological examples as well as experimental data (Patiño Douce and McCarthy, 1998) indicate that S-type granites would be formed in response to compression, collision and crustal thickening or post-orogenic extension, such as in the Palaeoproterozoic Svecofennian orogen of SW Finland (Väisänen et al., 2000), the Caledonian orogen of East Greenland (Kalsbeek et al., 2001), the European Hercynian belt (Ramírez and Grundvig, 2000), the Pan-African orogen (Jung et al., 2001), the Alps and Himalayas (Sylvester, 1998), the Andes of South America (Pimentel et al., 1999), the Eastern Australia (Allen et al., 1998) and early Proterozoic intra-continental compressional and collisional orogen in western Laurentia (De et al., 2000). Therefore, the occurring of S-type granites may be considered to be a petrological record of collisional and orogenic events between two plates or in intra-continent. The major heat source causing crustal anatexis to generate S-type granites includes radiogenic heating elements in thickening crust or upwelling asthenospheric mantle, underplating basaltic magma following subducting slab detachment and lithospheric delamination (Sylvester, 1998) during post-orogenic extension. However, A-type

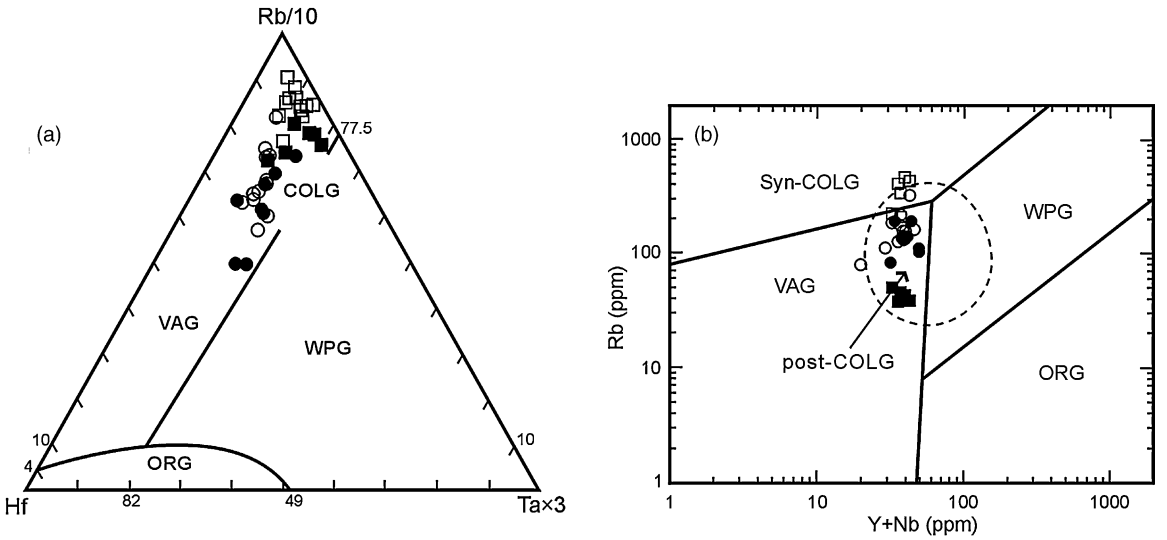

Fig. 6. Tectonic discriminative diagrams for the Neoproterozoic granites from Northern Guangxi. (a) Rb/10-Hf-Ta × 3 plot (after Harris et al., 1986); (b) (Y + Nb)-Rb plot (after Pearce et al., 1984) with field for post-collision granites (post-COLG) from Pearce (1996). Circle–granodiorites; Square–granites. Solid circle and square, this study; Open circle and square, data from Li XH et al. (2003) and Ge et al. (2001a).

granites only occur in crustal thinning setting (Patiño Douce and McCarthy, 1998). The granites related with mantle plume magmatism are anorogenic (Hamilton et al., 1998; Meighan et al., 1992), intraplate (Hames et al., 2000; Fröster et al., 1997; Ewart et al., 1998; Hofmann et al., 2000) and A-type granites (Vernikovsky et al., 2003; Ukstins et al., 2000), rather than S-type granites.

In fact, the S-type granitoids in Northern Guangxi are mostly probably related to the collision event between the Yangtze and Cathysia blocks as shown in the tectonically discriminant diagrams. For example, they exclusively fall within the collision granite field on Rb/10-Hf-Ta × 3 diagram (Fig. 6a) and the field of post-collisional granite on (Y + Nb) versus Rb diagram (Fig. 6b), implying a post-collisional (Liégeois, 1998) dynamic setting. In light of our new LA-ICP-MS U-Pb zircon dating results, the ages of the Neoproterozoic granites in Northern Guangxi show a broad range of ca. 35 million years from 835 Ma (the Zhaigun pluton) to 800 Ma (the Tianpeng pluton). The coeval nature of both the mafic and silicic magmatism (Li ZX et al., 2003) is somewhat questionable because the Sanfang pluton (804.3 ± 5.2 Ma) intruded and post-dated the 828 ± 7 Ma Yangmeiao mafic rocks (Li et al., 1999; Mao and Du, 2001), by up to 25 million years. A broad duration of igneous activity reflecting predominantly crustal melting is not directly consistent with predictions of mantle plume-driven magmatism.

The Neoproterozoic mafic-ultramafic rocks in Northern Guangxi were thought to be coeval with the Neoproterozoic S-type granites, and to be of mantle plume origin by Li et al. (1999), similar to the plume-related GDS in central-southern Australia (Zhao et al., 1994). Mantle plumes, in contrast to 'normal' mantle upwelling, are predicted to generate large volume mafic-dominated magma, erupted within 1–5 million years (MacKenzie and Bickle, 1988; Campbell and Griffiths, 1990; White and McKenzie, 1995; Condie, 2001), such as the Columbia River Flood Basalt (173,000 km^3) (Chesley and Ruiz, 1998), Siberia Trap (150,000 km^3) (Lightfoot et al., 1993), Deccan Traps (500,000 km^2) (Chandrasekharam, 2003), Willouran province of Australia (210,000 km^2) (Zhao et al., 1994) and so on. However, there are only ca. 100 km^2 for the Neoproterozoic mafic-ultramafic rocks in the study area (Zhao et al., 1987). These rocks have clearly arc geochemical features, not resembling with continental flood basalts and ocean island basalts (Zhou et al., 2004). Moreover, the Zhaigun granitic pluton (836 ± 2.4 Ma) intruded a mafic intrusion as mentioned above, suggesting a mafic magmatism interval of at least ca. 20 million years from 835 to 812 Ma (the Hejiawan layered diabases). This duration of mafic magmatisms in Northern Guangxi may also conflict with the mantle plume model.

6.2. *Neoproterozoic post-collisional events in Northern Guangxi*

Post-collisional extension due to delamination of the lithosphere after collision or collapse of the thickened orogen has been suggested as a viable model for crustal melting (e.g., Davies and Blanckenburg,

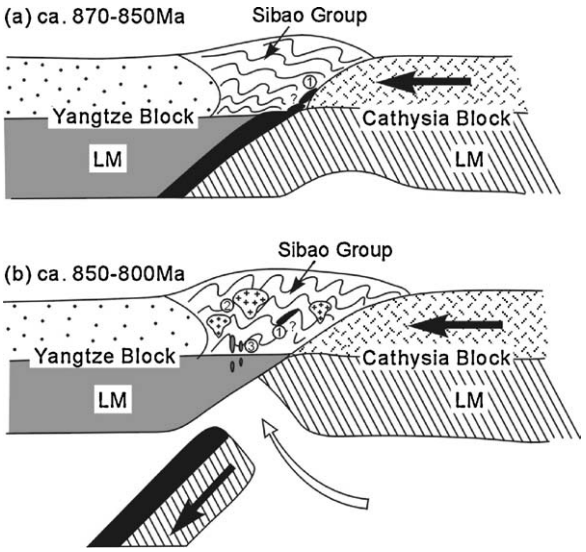

Fig. 7. Cartoons depicting the tectono-magmatic evolution of Northern Guangxi, South China. LM, lithosphere. (1) Possible relict oceanic crust; (2) granitic plutons; (3) mafic-ultramafic intrusions.

1995). Bonin et al. (1998) discussed the nomenclature of post-collisional magmatism and concluded that post-collisional episode would take place after the major collisional stage, but still during intra-continental plate convergence. It would be followed by the entirely intraplate post-orogenic episode (Liégeois, 1998; Väisänen et al., 2000). Geochronological studies of the high-pressure metamorphic blueschists from the eastern part of the Jiangnan orogen suggested that the collision peak happened in 870–850 Ma (Xu et al., 1992; Shu et al., 1993; Zhao and Cawood, 1999). The 835–800 Ma S-type granites and the mafic rocks in Northern Guangxi, therefore, are post-collisional and orogeny-related. In effect, nearly coeval S-type granites and mafic rocks association is atypical of mantle plumes. It may also occur within post-collisional setting (Bonin, 2004), such as in the Palaeoproterozoic Svecofennian Orogen of SW Finland (Väisänen et al., 2000) and the central-eastern Southern Alps, Italy (Rottura et al., 1998).

A preliminary simple evolution model for the generation of the Neoproterozoic igneous rocks in Northern Guangxi is shown in Fig. 7. The collision peak along the Jiangnan orogen happened in ca. 870–850 Ma (Fig. 7a). The collision process led to the folding of the W-E trending Sibao Group and the production of the 866 ± 14 Ma (Shu et al., 1993) high-pressure glaucophane-bearing schists at the eastern part of the Jiangnan orogen. After the collision peak, the breakoff of subducting lithospheric slab occurred as a natural consequence of an ocean closure (Davies and Blanckenburg, 1995; Fig. 7b). During the post-collisional episode in ca. 850–800 Ma, the subducting lithosphere detached and sank into the mantle (Fig. 7b). The gap was filled with deep mantle material, which provided heat causing melts generation in the overriding lithosphere and the continental crust.

6.3. Implications for the position of South China in Rodinia

It is insufficient and indecisive to discuss tectonic environments and evolutions based on geochronology merely. However, the large amount of the existing geochemical and geochronological data with our new dating results for the Neoproterozoic igneous rocks around the Yangtze Block make us accessible to study the position of South China in Rodinia. Ten spot analyses from zircon cores and two single zircon xenoliths yielded early Neoproterozoic ages ranging from ca. 870 to 950 Ma (Table 1). These ages overlap the timing of subduction-related arc magmatisms in the eastern part of the Jiangnan orogen: the 912–857 Ma (Wang, 2000) volcanic rocks of Shuangxiwu Group in Zhejiang Province. This indicates that subduction-related arc igneous or volcano-sedimentary materials of ca. 950–870 Ma might exist in the crustal basement in Northern Guangxi. If we accept the collision peak of the Jiangnan orogen occurred at ca. 870 Ma (Shu et al., 1993), the continent–continent collisional orogenic event along the orogen might span ca. 70 million years from 870 to 800 Ma (Tianpeng pluton in Northern Guangxi).

Combined with previous geochronological data for the ophiolites emplaced in arc or back-arc setting (ca. 1.0–0.96 Ga, Chen et al., 1991; Zhou et al., 1989; Zhou and Zhu, 1993; Li et al., 1994) and distributed along the eastern part of the Jiangnan orogen, the subducting events along southeastern margin of Yangtze block might last for ca. 130 million years (from ca. 1.0 to 0.87 Ga). As discussed by Zhou et al. (2002) and Zhao and Cawood (1999), the long duration of subduction might indicate that Yangtze Block must have been an isolated continent during the typical Grenvillian-age orogeny (ca. 1.3–1.0 Ga, McLelland et al., 1996) that led to the assembly of Rodinia. So, South China should not be placed at an interior position in Rodinia as Li ZX et al. (1995, 1999, 2003) proposed, but might flank its margin. In addition, the 835–812 Ma mafic rocks in Northern Guangxi have neither similarities with GDS in southeastern Australia in terms of geochemistry (Zhou et al., 2004), nor overlap in age, arguing against its position between eastern Australia and Laurentia put forward by Li et al. (1995). The 865–760 Ma arc magmatism (Zhou et al., 2002) in the western margin of the Yangtze Block is similar to

those of west-central Madagascar (Handke et al., 1999) and Seychelles Islands (Ashwal et al., 2002) that were located at the western margin of Rodinia. All of these evidence suggested that South China was probably adjacent to the northwestern Australia and India as some scholars proposed (Zhang and Piper, 1997; Evans et al., 2000; Li et al., 2004; Macouin et al., 2004).

7. Conclusion

The principal conclusions of this study are as follows:

1. New LA-ICP-MS U-Pb zircon dating reveals ca. 35 million years duration of magmatic activities in Northern Guangxi of South China. For the origin of Neoproterozoic igneous rocks in the area, orogenic, rather than mantle plume or superplume, model is preferred. The collision peak between the Yangtze and Cathysia blocks happened in ca. 870–850 Ma. The 835–800 Ma granitoids and mafic rocks in Northern Guangxi are post-collisional.
2. The geochemistry of the granitoids reveals typical S-type granite features. They formed in collision-related tectonic settings. Upwelling of deep mantle after the detachment of subducted slab provided heat source. The decompression due to the delamination of thickened lithosphere after collision led to the partial melting of the continental crust.
3. New La-ICP-MS U-Pb zircon dating results, combined with other geological evidence, indicate that South China might have been located at the west margin of the Rodinia supercontinent during the period ca. 870–800 Ma.

Acknowledgements

This research was financially supported by National Natural Science Foundation of China (grant nos. 40572039 and 40221301) and the Postgraduate Training Project of Jiangsu Province. We appreciate Prof. X.M. Zhou for providing a chance to LA-ICP-MS U-Pb zircon dating and C.R. Diwu for the assistance of analyses of LA-ICP-MS U-Pb zircon geochronology. Dr. S. Bryan is thanked for his constructive comments and grammatical corrections on the first version of the manuscript. This paper is greatly benefited from the constructive reviews by two reviewers and the profitable discussions with Profs. B. Bonin, W.Z. Shen, X. Wang, L.S. Shu, Y.F. Zheng, X.H. Li and F.Y. Wu.

References

Allen, C.M., Willianms, I.S., Stephens, C.J., Fielding, C.R., 1998. Granite genesis and basin formation in an extensional setting: the magmatic history of the northernmost New England Orogen. Aust. J. Earth Sci. 45, 875–888.

Andersen, T., 2002. Correction of common lead in U–Pb analyses that do not report ^{204}Pb. Chem. Geol. 192, 59–79.

Ashwal, L.D., Demaiffe, D., Torsvik, T.H., 2002. Petrogenesis of Neoproterozoic granitoids and related rocks from the Seychelles: the case for an Andean-type arc origin. J. Petrol. 43, 45–83.

BGMRGX (Bureau of Geology and Mineral Resources of Guangxi province), 1985. Regional Geology of Guangxi Autonomous Region. Geological Publishing House, Beijing, 1–853 (in Chinese with English abstract).

Black, L.P., Kamo, S.L., Williams, I.S., Mundil, R., Davis, D.W., Korsch, R.J., Foudoulis, C., 2003. The application of SHRIMP to Phanerozoic geochronology: a critical appraisal of four zircon standards. Chem. Geol. 200, 171–188.

Bonin, B., 2004. Do coeval mafic and felsic magmas in post-collisional to within-plate regimes necessarily imply two contrasting, mantle and crustal, sources? A review. Lithos 78, 1–24.

Bonin, B., Sekkal, A.A., Bussy, F., Ferrag, S., 1998. Alkali-calcic and alkaline post-orogenic (PO) granite magmatism: petrologic constraints and geodynamic settings. Lithos 45, 45–70.

Bryan, S.E., Riley, T.R., Jerram, D.A., Stephens, C.J., Leat, P.T., 2002. Silicic volcanism: an undervalued component of large igneous provinces and volcanic rifted margins. In: Menzies, M.A., Klemperer, S.L., Ebinger, C.J., Baker, J. (Eds.), Magmatic Rifted Margins, 362. Geological Society of America Special Paper, pp. 99–120.

Campbell, I.H., Griffiths, R.W., 1990. Implications of mantle plume structure for the evolution of flood basalts. Earth Planet. Sci. Lett. 99, 79–93.

Chandrasekharam, D., 2003. Deccan flood basalts. J. Geol. Soc. India Mem. 53, 30–54.

Chappell, B.W., White, A.J.R., 1974. Two contrasting granite types. Pac. Geol. 3, 173–174.

Chen, J.F., Foland, K.A., Xing, F.M., Xu, X., Zhou, T.X., 1991. Magmatism along the southeast margin of the Yangtze block: Precambrian collision of the Yangtze and Cathysia blocks of China. Geology 19, 815–818.

Chen, J.F., Jahn, B.M., 1998. Crustal evolution of southeastern China: evidence from Sr, Nd and Pb isotopic compositions of granitioids and sedimentary rocks. Tectonophysics 284, 101–133.

Chen, Y.C., Mao, J.W., Zou, T.R., 1995. Metallogenic Series of Ore Deposits and Metallogenic Evolution through Geological History in North Guangxi. Guangxi Science and Technology Press, Nanning, pp.1–433 (in Chinese).

Chesley, J.T., Ruiz, J., 1998. Crust–mantle interaction in large igneous provinces: implications from the Re–Os isotope systematics of the Columbia River flood basalts. Earth Planet. Sci. Lett. 154, 1–11.

Clemens, J.D., 2003. S-type granitic magmas—petrogenetic issues, models and evidence. Earth Sci. Rev. 61, 1–18.

Condie, K.C., 2001. Mantle Plumes and their Records in Earth History. Cambridge University Press, Oxford, UK, pp.1–306.

Davies, J.H., Blanckenburg, F.V., 1995. Slab breakoff: A model of lithosphere detachment and its test in the magmatism and deformation of collisional orogens. Earth Planet. Sci. Lett. 129, 85–102.

De, S.K., Chacko, T., Creaser, R.A., Muehlenbachs, K., 2000. Geochemical and Nd-Pb-O isotope systematics of granites from the

Taltson Magmatic zone, NE Alberta: implications for early Proterozoic tectonics in western Laurentia. Precam. Res. 102, 221–249.

Evans, D.A.D., Li, Z.X., Kirschvink, J.L., Wingate, M.T.D., 2000. A high-quality mid-Neoproterozoic paleomagnetic pole from South China, with implications for ice ages, regional stratigraphy, and the breakup configuration of Rodinia. Precam. Res. 100, 313–334.

Ewart, A., Milner, S.C., Armstrong, R.A., et al., 1998. Etendeka volcanism of the Goboboseb Mountains and Messum igneous complex, Namibia. 1. Geochemical evidence of early Cretaceous Atristan plume melts and the role of crustal contamination in the Paraná-Etendeka CFB. J. Petrol. 39, 191–225.

Franzini, M., Leoni, L., Saitta, M., 1972. A simple method to valuate the matrix effect in X-ray fluorescence analysis. X-ray Spectrom. 1, 151–154.

Fröster, H.J., Tischendorf, G., Trumbull, R.B., 1997. An evaluation of the Rb vs (Y+Nb) discrimination diagram to infer tectonic setting of silicic igneous rocks. Lithos 40, 261–293.

Ge, W.C., Li, X.H., Li, Z.X., Wang, J., Zhou, H.W., Li, J.Y., 2000. Geological and geochemical evidence for the genesis of the tremolitized mafic rocks from Baotan in northern Guangxi. Geochimica 29, 253–258 (in Chinese, with English Abstr.).

Ge, W.C., Li, X.H., Li, Z.X., Zhou, H.W., Li, J.Y., 2001a. Geochemical studies on two types of Neoproterozoic peraluminous granitoids in northern Guangxi. Geochimica 30 (1), 24–34.

Ge, W.C., Li, X.H., Liang, X.R., Wang, R.C., Li, Z.X., Zhou, H.W., 2001b. Geochemistry and geological implications of mafic-ultramafic rocks with the age of ~825 Ma in Yuanbaoshan-Baotan area of northern Guangxi. Geochimica 30, 123–130 (in Chinese, with English Abstr.).

GXRGST(Guangxi Regional Geological Survey Team), 1987. Regional Geological Survey Report (Baotan area, 1:50000), 1–294 (in Chinese).

GXRGST (Guangxi Regional Geological Survey Team), 1995. Regional Geological Survey Report (Sanfang area, 1:50000), 1–225 (in Chinese).

Guo, L.Z., Shi, Y.S., Ma, R.S., 1980. The geotectonic framework and crustal evolution of South China. In: Scientific Paper on Geology for International Exchange. J. Geological Publishing House, Beijing, pp. 109–116 (in Chinese, with English Abstr.).

Hames, W.E., Renne, P.R., Ruppel, C., 2000. New evidence for geologically instantaneous emplacement of earliest Jurassic Central Atlantic magmatic province basalts on the North American margin. Geology 28, 859–862.

Hamilton, M.A., Pearson, D.G., Thompson, R.N., et al., 1998. Rapid eruption of Skye lavas inferred from precise U-Pb and Ar-Ar dating of the Rum and Cuillin plutonic complexes. Nature 394, 260–263.

Han, F., Shen, J.Z., Nie, F.J., Li, S.C., Yang, K.T., Yang, C., Ding, X.S., 1994. The geochronical studies of Sibao Group in the southern margin of Jiangnan massif. Acta Geoscientia Sinica, 43–50 (in Chinese, with English Abstr.).

Handke, M.J., Tucker, R.D., Ashwal, L.D., 1999. Neoproterozoic continental arc magmatism in west-central Madagascar. Geology 27, 351–354.

Harris, N.B.W., Pearce, J.A., Tindle, A.G., 1986. Geochemical characteristics of collision-zone magmatism. In: Coward, M.P., Ries. A.C. (Eds.), Collision Tectonics, Vol. 19. Geol. Soc. Spec. Publ., pp. 67–81.

Hofmann, C., Féraud, G., Courtillot, V., 2000. $^{40}Ar/^{39}Ar$ dating of mineral separates and whole rocks from the western Ghats lava pile: further constraints on duration and age of the Deccan traps. Earth Planet. Sci. Lett. 180, 13–27.

Jackson, S.E., Pearson, N.J., Griffin, W.L., Belousova, E.A., 2004. The application of laser ablation-inductively coupled plasma-mass spectrometry to in situ U–Pb zircon geochronology. Chem. Geol. 211, 47–69.

Jiang, G.Q., Sohl, L.E., Blick, N.C., 2003. Neoproterozoic stratigraphic comparison of the Lesser Himalaya (India) and Yangtze block (South China): paleogeographic implications. Geology 31, 917–920.

Jung, S., Mezger, K., Hoernes, S., 2001. Trace element and isotopic (Sr, Nd, Pb, O) arguments for a mid-crustal origin of Pan-African garnet-bearing S-type granites from the Damara orogen (Namibia). Precam. Res. 110, 325–355.

Kalsbeek, F., Jepsen, H.F., Nutman, A.P., 2001. From source migmatites to plutons: tracking the origin of ca. 435 Ma S-type granites in the East Greenland Caledonian orogen. Lithos 57, 1–21.

Li, X.H., Zhao, Z.H., Gui, X.T., Yu, J.S., 1991. Sm-Nd isotopic and zircon U-Pb constraints on the age of formation of the Precambrian crust in southeast China. Geochimica 3, 255–264 (in Chinese, with English Abstr.).

Li, X.H., 1999. U-Pb zircon ages of granites from the southern margin of the Yangtze margin: timing of Neoproterozoic Jinning Orogen in SE China and implication for Rodinia assembly. Precam. Res. 97, 43–57.

Li, X.H., Li, Z.X., Ge, W.C., Zhou, H.W., Li, W.X., Liu, Y., Wingate, M.T.D., 2003a. Neoproterozoic granitoids in South China: crustal melting above a mantle plume at ca. 825 Ma? Precam. Res. 122, 45–83.

Li, X.H., Zhou, G.Q., Zhao, J.X., Fanning, C.M., Compston, W., 1994. SHRIMP iron microprobe zircon U-Pb age of the NE Jiangxi ophiolite and its tectonic implications. Geochemica 23, 125–131 (in Chinese, with English Abstr.).

Li, Z.X., Evans, D.A.D., Zhang, S., 2004. A 90° spin on Rodinia: possible causal links between the Neoproterozoic supercontinent, superplume, true polar wander and low-latitude glaciation. Earth Planet. Sci. Lett. 220, 409–421.

Li, Z.X., Li, X.H., Kinny, P.D., Wang, J., 1999. The breakup of Rodinia: did it start with a mantle plume beneath South China? Earth Planet. Sci. Lett. 173, 171–181.

Li, Z.X., Li, X.H., Kinny, P.D., Wang, J., Zhang, S., Zhou, H.W., 2003b. Geochronology of Neoproterozoic syn-rift magmatism in the Yangtze Craton, South China and correlations with other continents: evidence for a mantle superplume that broke up Rodinia. Precam. Res. 122, 85–109.

Li, Z.X., Zhang, L.H., Powell, C.M., 1995. South China in Rodinia: a part of the missing link between Australia-east Antarctica and Laurentia? Geology 23, 407–410.

Liégeois, J.P., 1998. Some words on the post-collisional magmatism. Lithos 45, xv–xvii.

Lightfoot, P.C., Hawkesworth, C.J., Hergt, J., Naldrett, A.J., Gorbachey, N.S., Fedorenko, V.A., Doherty, W., 1993. Remobilisation of the continental lithosphere by a mantle plume: major-, trace-element, and Sr-, Nd and Pb-isotope evidence from picritic and tholeiitic lavas of the Noril'sk District. Mexico Contrib. Mineral. Petrol. 114, 171–188.

Ling, W.L., Gao, S., Zhang, B.R., Li, H.M., Liu, Y., Cheng, J.P., 2003. Neoproterozoic tectonic evolution of the northwestern Yangtzecraton, South China: implications for amalgamation and break-up of the Rodinia Supercontinent. Precam. Res. 122, 111–140.

Liu, C.S., Ling, H.F., Xiong, X.L., Shen, W.Z., Wang, D.Z., Huang, X.L., Wang, R.C., 1999. An F-rich Sn-bearing volcanic-intrusive complex in Yanbei, South China. Econ. Geol. 94, 325–342.

Ludwig, K.R., 1991. ISOPLOT: A plotting and regression program for radiogenic-isotope data. U.S. Geological Survey Open-file Report, 39.

MacKenzie, D.P., Bickle, M.J., 1988. The volume and composition of melt generated by extension of the lithosphere. J. Petrol. 29, 625–679.

Macouin, M., Besse, J., Ader, M., Gilder, S., Yang, Z., Sun, Z., Agrinier, P., 2004. Combined paleomagnetic and isotopic data from the Doushantuo carbonates, South China: implications for the "snowball Earth" hypothesis. Earth Planet. Sci. Lett. 224, 387–398.

Mao, J.W., Du, A.D., 2001. Re-Os isotopic age of Cu-Ni sulphide ore in Baotan area of northern Guangxi and its geological significance. Sci. China (Ser. D) 31, 992–998 (in Chinese).

McLelland, J., Daly, J.S., McLelland, J.M., 1996. The Grenville Orogenic Cycle (ca. 1350-1000 Ma): an Adiron-dack perspective. Tectonophysics 265, 1–28.

Meighan, I.G., Fallick, A.E., McCormick, A.G., 1992. Anorogenic granite magma genesis: new isotopic data for the southern sector of the British Tertiary igneous province. T Roy. Soc. Edin. Earth Sci. 83, 227–233.

Patiño Douce, A.E., McCarthy, T.C., 1998. Melting of crustal rocks during continental collision and subduction. In: Hacker, B.R., Liou, J.G. (Eds.), When Continents Collide: Geodynamics and Geochemistry of Ultrahigh-Pressure Rocks. Kluwer Academic Publishers.

Pearce, J.A., 1996. Sources and settings of granitic rocks. Episodes 19, 120–125.

Pearce, J.A., Harris, N.B.W., Tindle, A.G., 1984. Trace element discrimination diagrams for the tectonic interpretation of granitic rocks. J. Petrol. 25, 956–983.

Pearce, N.J.G., Perkins, W.T., Westgate, J.A., et al., 1997. A compilation of new and published major and trace element data for NIST SRM 610 and NIST SRM 612 glass reference materials. Geostand. Newslett. 21, 115–144.

Pimentel, M.M., Fuck, R.A., Botelho, N.F., 1999. Granites and the geodynamic history of the neoproterozoic Brasília belt, Central Brazil: a review. Lithos 46, 463–483.

Ramírez, J.A., Grundvig, S., 2000. Cause of geochemical diversity in peraluminous granitic plutons: the Jálama pluton, Central-Iberian zone (Spain and Potugal). Lithos 50, 171–190.

Rottura, A., Bargossi, G.M., Caggianelli, A., Moro, A.D., Visonà, D., Tranne, C.A., 1998. Origin and significance of the Permian high-K calc-alkaline magmatism in the central-eastern Southern Alps, Italy. Lithos 45, 329–348.

Shu, L.S., Zhou, G.Q., Shi, Y.S., Yin, J., 1993. Study of high pressure metamorphic blueschist and its late Proterozoic age in the eastern Jiangnan belt. Chin. Sci. Bull. 38, 1779–1882 (in Chinese).

Sylvester, P.J., 1998. Post-collisional strongly peraluminous granities. Lithos 45, 29–44.

Ukstins, I.A., Baker, J., Al-Kadasi, M., et al., 2000. Voluminous explosive silicic eruptions during Oligocene flood volcanism in Yemen. Royal Holloway, University of London, Department of Geology, Penrose. Volcanic rifted margins, Abstracts 85.

Väisänen, M., Mänttäri, I., Kriegsman, L.M., Hölttä, P., 2000. Tectonic setting of post-collisional magmatism in the Palaeoproterozoic Svecofennian Orogen, SW Finland. Lithos 54, 63–81.

Vernikovsky, V.A., Pease, V.L., Vernikovskaya, A.E., Romanov, A.P., Gee, D.G., Travin, A.V., 2003. First report of early Triassic A-type granite and syenite intrusions from Taimyr: product of the northern Eurasian superplume? Lithos 66, 22–36.

Wang, J., 2000. Neoproterozoic Rifting History of South China: Significance to Rodinia Breakup. Geological Publishing House, Beijing (in Chinese, with English Abstr.).

Wang, X.L., Zhou, J.C., Qiu, J.S., Gao, J.F., 2004a. Comment on 'Neoproterozoic granitoids in South China: crustal melting above a mantle plume at ca. 825Ma?' by Xian-Hua Li et al. (PR 122, 45–83, 2003). Precam. Res. 122, 401–403.

Wang, X.L., Zhou, J.C., Qiu, J.S., Gao, J.F., 2004b. Geochemistry of the Meso- to Neoproterozoic basic-acid rocks from Hunan Province, South China: implications for the evolution of the western Jiangnan orogen. Precam. Res. 135, 79–103.

White, R.S., McKenzie, D., 1995. Mantle plumes and flood basalts. J. Geophys. Res. 100, 543–585.

Wiedenbeck, M., Alle, P., Corfu, F., et al., 1995. Three natural zircon standards for U–Th–Pb, Lu–Hf, trace element and REE analyses. Geostand. Newslett. 19, 1–23.

Xu, B., Guo, L.Z., Shi, Y.S., 1992. Proterozoic Terranes and Multiphase Collision Orogens in Anhui-Zhejiang-Jiangxi areas. Geological Publishing House, Beijing, pp. 1–112 (in Chinese, with English Abstr.).

Xu, X.S., Zhou, X.M., 1992. Precambrian S-type granitoids in South China and their geological significance. Journal of Nanjing University (Natural sciences edition) 28, 423–430 (in Chinese, with English Abstr.).

Yan, D.P., Zhou, M.F., Song, H.L., Malpas, J., 2002. Where was South China located in the reconstruction of Rodinia? Earth Sci. Frontiers 9, 249–256 (in Chinese with English abstract).

Yang, L.Z., 1990. Middle Proterozoic komatiite in northern Guangxi. Region. Geol. China 1, 14–22 (in Chinese with English abstract).

Ye, S., Yang, M., Ye, D.L., Tai, D.Q., Ren, Y.X., 2001. Rb-Sr isotopic dating and significance of kimberlitic lamprophyre pipe from Lujing, Anyuan, Jiangxi province. Geol. Sci. Technol. Inform. 20, 27–29 (in Chinese with English abstract).

Yuan, H.L., Wu, F.Y., Gao, S., Liu, X.M., Xu, P., Sun, D.Y., 2003. Determination of U-Pb age and rare earth element concentrations of zircons from Cenozoic intrusions in northeastern China by laser ablation ICP-MS. Chin. Sci. Bull. 48, 2411–2421.

Zhang, Q.R., Piper, J.D.A., 1997. Palaeomagnetic study of Neoproterozoic glacial rocks of the Yangzi Block: palaeolatitude and configuration of South China in the late Proterozoic Supercontinent. Precam. Res. 85, 173–199.

Zhao, G.C., Cawood, P.A., 1999. Tectonothermal evolution of the Mayuan assemblage in the Cathaysia Block: implications for Neoproterozoic collision-related assembly of the South China craton. Am. J. Sci. 299, 309–339.

Zhao, J.X., McCulloch, M.T., Korsch, R.J., 1994. Characterisation of a plume related ~800 Ma magmatic event and its implication for basin formation in central southern Australia. Earth Planet. Sci. Lett. 121, 349–367.

Zhao, Z.J., Ma, D.Q., Lin, H.K., Yuan, C.L., Zhang, X.H., 1987. A study on the Precambrian granitoids from Bendong and Sanfang massifs, Northern Guangxi, In: Yichang Institute of Geology, Mineral, Resources, Research Reports of the Geology, Mineral, pp. 1–27 (in Chinese, with English Abstr.).

Zheng, Y.F., 2004. Position of South China in configuration of Neoproterozoic supercontinent. Chin. Sci. Bull. 49, 751–753.

Zhou, J.C., Wang, X.L., Qiu, J.S., Gao, J.F., 2004. Geochemistry of Meso- and Neoproterozoic mafic-ultramafic rocks from northern Guangxi, China: arc or plume magmatism? Geochem. J. 38, 139–152.

Zhou, M.F., Yan, D.P., kennedy, A.K., Li, Y.Q., Ding, J., 2002. SHRIMP U-Pb zircon geochronological and geochemical evidence

for Neoproterozoic arc-magmatism along the western margin of the Yangtze Block, South China. Earth Planet. Sci. Lett. 196, 51–67.

Zhou, M.F., Zhao, T.P., Malpas, J., Sun, M., 2000. Crustal-contaminated komatiitic basalts in southern China: products of a Proterozoic mantle plume beneath the Yangtze block. Precam. Res. 103, 175–189.

Zhou, X.M., Zhu, Y.H., 1993. Petrological evidences of Neoproterozoic collision-orogenic and suture belts in southeastern China. In: Li, J.L. (Ed.), Lithospheric Structures and Geological Evolution in Continent from Southeastern China. Metallurgical industry Press, Beijing, pp. 87–97 (in Chinese).

Zhou, X.M., Zou, H.B., Yang, J.D., Wang, Y.X., 1989. Sm-Nd isochronous age of Fuchuan ophiolite suite in Shexian county, Anhui Province, and its geological significance. Chin. Sci. Bull. 35, 208–212.

Zhu, J.C., Li, R.L., Li, F.C., Xiong, X.L., Zhou, F.Y., Huang, X.L., 2001. Topaz-albite granites and rare-metal mineralization in the Limu distract, Guangxi Province, southeast China. Mineralium Deposita 36, 393–405.